CRYOSPHERIC GEOMORPHOLOGY: Dating Glacial Landforms I: archival, incremental, relative dating techniques and age-equivalent stratigraphic markers

Bethan J. Davies[1]*

[1]Centre for Quaternary Research, Department of Geography, Royal Holloway University of London, Egham Hill, Egham, Surrey, TW20 0EX

*Bethan.davies@rhul.ac.uk

Manuscript Code: 40019

Abstract

Combining glacial geomorphology and understanding the glacial process with geochronological tools is a powerful method for understanding past ice-mass response to climate change. These data are critical if we are to comprehend ice mass response to external drivers of change and better predict future change. This chapter covers key concepts relating to the dating of glacial landforms, including absolute and relative dating techniques, direct and indirect dating, precision and accuracy, minimum and maximum ages, and quality assurance protocols. The chapter then covers the dating of glacial landforms using archival methods (documents, paintings, topographic maps, aerial photographs, satellite images), relative stratigraphies (morphostratigraphy, Schmidt hammer dating, amino acid racemization), incremental methods that mark the passage of time (lichenometry, dendroglaciology, varve records), and age-equivalent stratigraphic markers (tephrochronology, palaeomagnetism, biostratigraphy). When used together with radiometric techniques, these methods allow glacier response to climate change to be characterized across the Quaternary, with resolutions from annual to thousands of years, and timespans applicable over the last few years, decades, centuries, millennia and millions of years. All dating strategies must take place within a geomorphological and sedimentological framework that seeks to comprehend glacier processes, depositional pathways and post-depositional processes, and dating techniques must be used with knowledge of their key assumptions, best-practice guidelines and limitations.

Keywords

Chronology, varves, tephrochronology, dendroglaciology, lichenometry, glacial landforms, Schmidt hammer

Glossary

Allochthonous	Rocks that have been transported & deposited (inc. erratics, alluvial fans, gelifluction, etc.
Autochthonous	Rocks that have remained at or near site of formation
Cryptotephra	Distal tephra deposits, preserved as glass shards in sedimentary archives.
Dipolar	The Earth's magnetic field is dipolar, with a north and south pole.
Ecesis time	The colonisation time lag interval on a surface; the time taken for trees, lichens or other species to colonise a surface.
Tephra	All-inclusive term for explosively erupted, loose, fragmental products of a volcanic eruption. Includes all grain sizes from find dust to large boulders.
Tephrochronology	The use of tephras as isochrones (time-parallel marker beds) to link stratigraphies in different localities. Enables the operator to establish relative or numerical ages.
Tephrostratigraphy	Study of sequences of tephra layers or strata and associated deposits and their relative and numerical ages.

Contents

1 Introduction

Over the last few decades, multiple methodologies for dating different types of glacial landform have become available to chronologists and geomorphologists (Benn and Owen, 2002; Briner, 2011; Davies et al., 2020; Jull, 2018; Kirkbride and Winkler, 2012; Lowe and Walker, 2014; Lüthgens and Böse, 2012; Small et al., 2017). There has been a progression from mostly relying on relative stratigraphies, such as the principal of superposition (e.g. Caldenius, 1932) and morphostratigraphy (Lüthgens and Böse, 2012), to radiocarbon dating to constrain the timing of deglaciation (e.g. Clapperton, 1995; Dyke et al., 2003; Mercer, 1972), and then on to a wide range of dating methodologies suitable for a range of different environments. These methods have become increasingly precise, refined and nuanced, and different approaches are now available to date different environments. New tools, such as varve chronologies and tephrochronology, offer ever more precise methods to constrain past glaciations in time, and provide a range of new methods in places that are commonly poor in organic materials.

In this chapter, the focus is on the broad application of varied chronological methods to glacial landforms. In most cases, the overall goal of the research project is to constrain in time the extent, thickness, rate of recession or some other property of a past or presently receded ice mass (Stokes et al., 2015). Therefore, most tools here are concerned with delimiting the ice margins (terminal or lateral moraines, glacier forelands, proglacial lacustrine sediments), either vertically or horizontally. Typically, this involves applying relative and absolute dating methods to glacial landforms formed at the ice margin, such as moraines or outwash terraces, or the timing of formation and duration of the existence of ice-dammed proglacial lakes, to yield the timing of past glaciation.

This broad review aims to provide an overview and introduction to the varied methods available for dating glacial landforms across different environments and timescales. It covers key concepts and theoretical requirements for each method, and considers the assumptions and likely best-practice applications of each method. It also considers quality assurance protocols for the most frequently applied methods. While there are many other chronological tools available, the ones covered here are commonly applied to dating glacial landforms.

This review first appraises some key concepts essential for dating glacial landforms, and then focuses on four key methods for dating past glacial environments. Firstly, archival methods include historical documents, maps, and remotely sensed images that allow a calendar year to be assigned to particular landforms. Secondly, relative dating methods such as morphostratigraphy, Schmidt hammer dating of boulders on moraines and amino acid racemization dating of *in situ* or reworked shells allow sequences to be placed into a relative order of age. Thirdly, incremental methods, including lichenometry on boulders or bedrock, dendroglaciology from trees associated with glacial landforms and varve records from glaciolacustrine or glacially influenced lakes, demark the incremental passage of time and can be used to provide a calendar age when calibrated. Finally, age-equivalent stratigraphic markers, including tephrochronology, palaeomagnetism and biostratigraphy, are based on contemporaneous horizons in separate and perhaps very different or very distally located environments (Lowe and Walker, 2014); these tools can be applied in some cases to very old sediments beyond the reach of many radiometric measurements. Radiometric dating techniques yielding numerical ages, including cosmogenic nuclide dating, radiocarbon dating, optically stimulated luminescence (OSL) and Argon/Argon dating, are covered in a separate chapter.

2 Key chronological concepts

2.1 Length of time for different chronometers

Different chronological tools are best applied for glacial landforms of different ages. The youngest landforms, that are expected to date from the last few hundred years, are best dated through historical documents and archives, lichenometry, dendrochronology, and relative dating tools such as Schmidt hammer dating. These tools work well for the last approximately decades to 1000 years, but reliability and applicability tends to break down after this. Radiocarbon dating works well for organic materials with an age of ~300 to ~40,000 years (Briner, 2011). Cosmogenic nuclide surface exposure dating can be applied to moraines only a few hundred years old (Schaefer et al., 2009) to those dating from glaciations in the middle to Late Pleistocene (Hein et al., 2017; Mendelová et al., 2020), with uncertainties of around 10%. Similarly, amino acid racemization of shells can cover a time period of 1000s of years to the Mid Pleistocene, but with larger uncertainties (Magee et al., 2009).

2.2 Absolute and relative dating techniques

The methods used for glacial landforms can loosely be categorized into either dating the exposure age (the time at which the landform was exposed to the atmosphere following the recession of ice), the burial age (the time elapsed since the deposit was buried), or the onset of organic sedimentation (the development of organic material following the recession of the ice). These methods include both absolute and relative dating techniques; here, absolute dating techniques rely on a chronometer, such as radioactive decay or the accumulation of a particular radionuclide, or another process that has a defined function over time (Jull, 2018). These methods include radiocarbon dating of organics associated directly with glacial landforms, cosmogenic nuclide exposure-age dating (the analysis of the accumulation of cosmogenic nuclides within the surface of a boulder or bedrock), optically stimulated luminescence dating of an outwash fan directly linked to a moraine, and so on.

Relative dating techniques rely on observations to mark the passage of time and put landforms into a relative order in terms of time since formation. These techniques include lichenometry (the comparison of lichen sizes to a growth curve), dendrochronology (the comparison and correlation of annual growth rings in a tree with established chronologies), and palaeomagnetic dating (the comparison of magnetically susceptible materials in sediments to known geomagnetic fluctuations).

2.3 Direct and indirect dating techniques

Dating techniques can be considered direct or indirect (Small et al., 2017). Direct dating (e.g. of an exposed glacially eroded surface) methods provide a direct minimum age for the landform in question and can be directly linked to past glacial extents. These methods usually date the exposure age of the landform. Indirect methods (e.g. of fluvioglacial outwash) will use ages to provide either a minimum, maximum, or ideally, bracketing ages for the landform. This could include, for example, radiocarbon dating basal organic sediments in small ponds inside and outside of a moraine, or bracketing Ar/Ar ages of lavas interbedded with moraines. The geochronological control on these features could represent either minimum or maximum ages, depending on the stratigraphic context (Small et al., 2017).

2.4 Different tools for different environments

The wide range of tools available means that a choice must be made about the most appropriate tool to date a particular landform (Figure 1). The first, and most important question, is the type of landform and the type of materials suitable for dating. Direct exposure age dating of moraines using cosmogenic nuclide dating requires the availability of a number of large boulders with a mineralogy suitable for extracting particular target nuclides (such as quartz, for ^{10}Be dating). Radiocarbon dating relies on the availability of organic material, either in kettle holes or small ponds directly associated with the moraine (which will provide a minimum age; the moraine must be older than the material), organic material interbedded within the moraine (which will provide a maximum age; the moraine must be younger than the organic material); or alternatively indirectly dating the landform with bracketing ages, such as from radiocarbon ages from basal organics from bogs or ponds both inside and outside the moraine. OSL dating can be applied to glaciofluvial outwash, but can only provide an age for the location of the ice margin if the outwash can be clearly geomorphologically related to a particular moraine. This method also requires the target minerals (quartz, feldspar) to have been appropriately bleached, which is not guaranteed in the commonly silty glaciofluvial environment (Lukas et al., 2007), and not all quartz grains are suitable. Varve chronologies require the presence of annually laminated sequences deposited in glaciolacustrine environments, and ideally should be able to be directly related to a moraine to locate an ice margin (e.g. Bendle et al., 2017).

The second question is the length of time since the landform was deposited or formed (Figure 1), and the level of precision required. This assumes that the landform and its associated sediments have not undergone significant reworking or post-depositional modification, exhumation, or burial. Together, these two processes determine the most appropriate chronological tool.

Choice of the correct geochronological tool requires a thorough understanding of the geomorphological and depositional context of the landform, post-depositional processes and modifications, as well as an understanding of glacial processes that will affect debris transport pathways and erosion (cf. Chandler et al., 2018). For this important reason, all dating campaigns should be strongly grounded in geomorphological mapping, focused on a strong understanding of the process. Related morphostratigraphy can help guide a dating campaign. Adopting a process-based landsystems approach to glacial landscapes (Bickerdike et al., 2018; Evans, 2007; Evans and Twigg, 2002) will significantly improve the successes of a dating campaign.

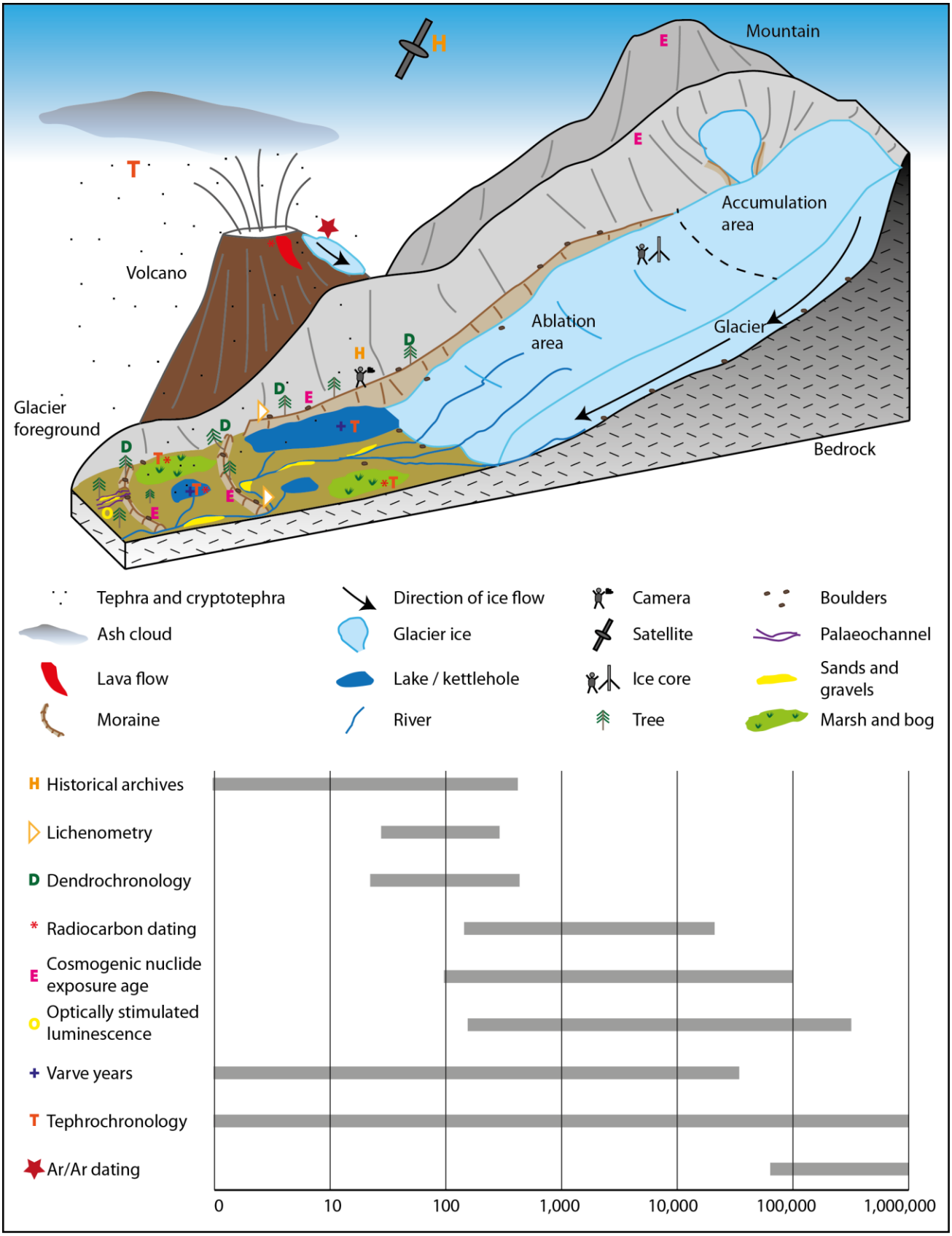

Figure 1. Cartoon illustrating applications and length of time applicable for various different methods for dating terrestrial glacial landforms.

2.5 Precision and accuracy

Precision and accuracy is a key consideration when dating past glacial environments. Numerical radiometric dating tools such as radiocarbon dating or cosmogenic nuclide exposure-age dating can give very precise ages, with errors of a few tens to few hundreds of years over the last 20,000 years. Here, the term 'precision' refers to the statistical uncertainty attached to any physical or chemical measurement (Lowe and Walker, 2014). However, numerical dating techniques must be carefully applied; these tools are also prone to giving inaccurate ages if poorly applied (Figure 2).

'Accuracy' refers to the degree of correspondence between the true age and that obtained through the dating process. Geological scatter in several numerical ages for one landform often far exceeds the precise analytical uncertainty, and this accuracy is much harder to quantify and identify. For example, radiocarbon dating can give inaccurate or biased ages if the radiocarbon reservoir in freshwater environments or contamination from older carbon is not taken into account. Likewise, boulders on moraines may contain inherited cosmogenic nuclides, which can produce an anomalously old age. Smaller boulders may be exhumed from the moraine during weathering and surface lowering of the moraine, producing anomalously young ages. It is therefore important not to take the very precise analytical ages derived at face value, but to carefully understand why and how they are applied, the potential sources of inaccuracy, and strategies for excluding outliers. Age reliability, a function of both the precision and the accuracy of the derived age, requires a knowledge of the contexts of deposition, taphonomy, and post-depositional processes (Lowe and Walker, 2014).

For this reason, any dating strategy should take place within a careful geomorphological framework and should be carefully grounded in glacier process. Detailed geomorphological mapping and an understanding of the glacial landsystem (Chandler et al., 2018; Evans, 2007, 2004) and landform morphostratigraphy (Boston et al., 2015; Lukas, 2006) is required to guide and inform any dating campaign. If these approaches are carefully followed, then sampled moraines can provide numerical ages that can be extrapolated to other valleys or locations (cf. Briner, 2011).

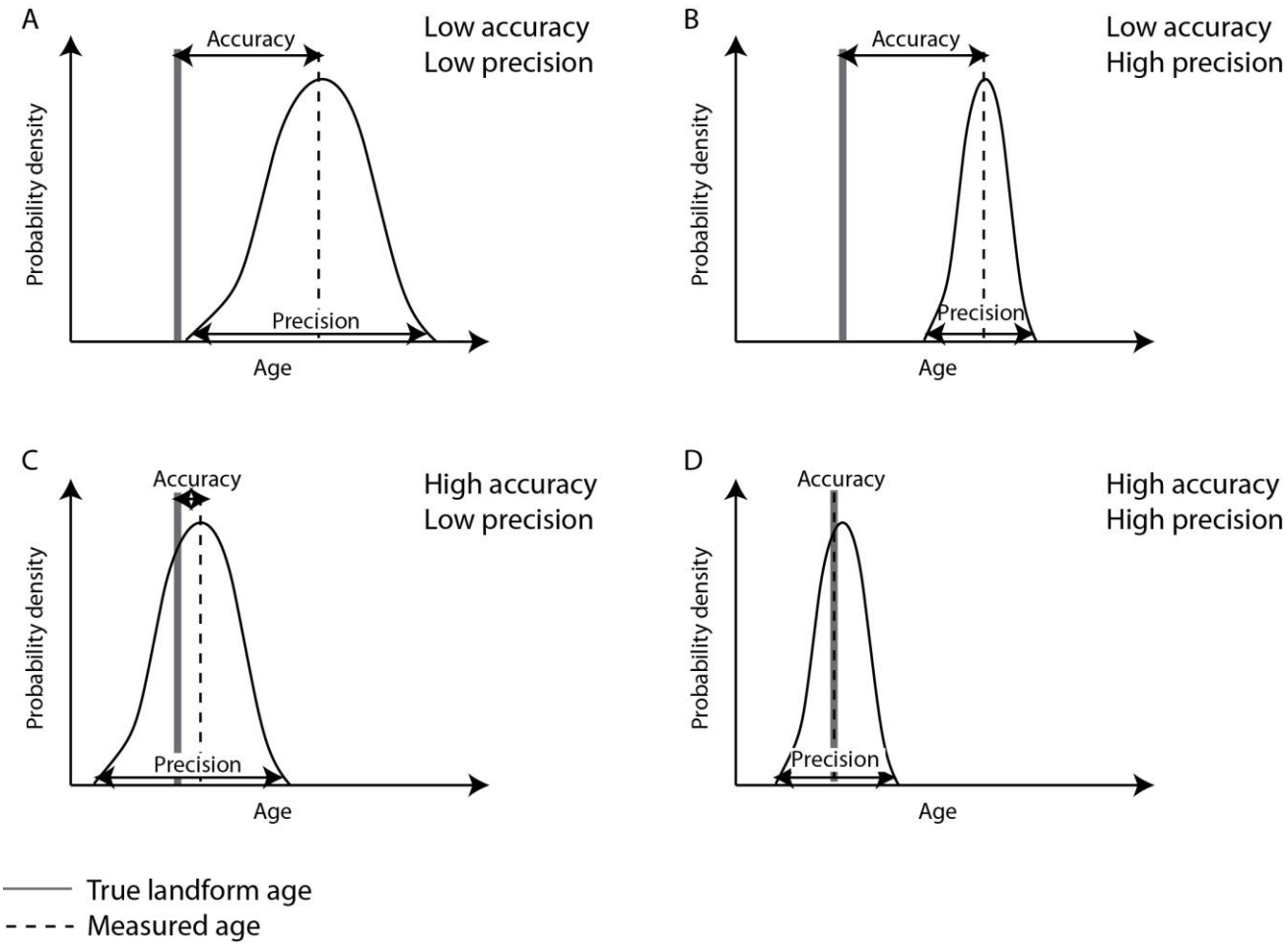

Figure 2. Cartoon illustrating precision and accuracy in dating glacial landforms. Dashed lines on the right show the measured age. Grey lines on the left show the 'true' age of the landform. Numerical ages may show wide geological scatter and may be offset from the moraine age (e.g. A). Many techniques have very narrow analytical uncertainties, which may return very precise ages, but they may not always be accurate (e.g. panel B). Only the panel C or, better, D, can provide a good estimate of the age of the landform.

2.6 Minimum and Maximum ages

Dating glacial landforms requires careful attention to stratigraphic principles. Ages related to glacial landforms can typically be divided into *minimum* or *maximum* ages. A minimum age indicates that the timing of the glaciation occurred after the event dated. For example, organic matter reworked into a moraine and radiocarbon date provides a minimum age for the formation of that moraine. A bog, mire or pond overlying the moraine, with basal sediments dated by radiocarbon or tephra, provides a bracketing maximum age for that moraine.

2.7 Quality assurance protocols

Once calculated, numerical ages in a study should be subjected to a quality assurance process. The method for this has been developed recently during systematic meta-analyses of published ages (Davies et al., 2020; Ely et al., 2019; Hughes et al., 2016; Small et al., 2017). Each method has a range of criteria against which

ages should be scored before a mean age for the landform can be calculated. Practitioners should be aware of these scoring criteria and should design studies appropriately, and reviewers and users of published data should assess published ages accordingly.

For all dating methodologies, high quality ages should have a clearly defined geomorphological and geological context, with a specified uncertainty, and the samples should appear *in situ* with a well understood depositional context. The text below provides brief additional quality assurance protocols for each dating methodology described.

3 Archival methods

3.1 Remote sensing

Aerial photographs are available for many places from the mid-Twentieth Century onwards, and can be used to determine glacier extent in the 1940s and 1950s (e.g. Harrison et al., 2007; O'Neel et al., 2019; Rabatel et al., 2013). The advent of satellite imagery in the 1970s and the development of Geographic Information Systems (GIS) has resulted in the development of the field of glacier inventory mapping. Each remotely sensed dataset (orthoimages and digital elevation models) provides a snapshot in time that immortalizes glacier extent. Digital elevation models can be used to assess surface elevation and hence glacier volume changes (e.g., Pritchard and Vaughan, 2007; Willis et al., 2012). Techniques for mapping glacier and glacier-lake extent and length from optical satellite imagery include automatic derivation of glacier outlines (Frey et al., 2010; Le Bris and Paul, 2013; Paul et al., 2013) and manual derivation or editing of shapefile polygons in a GIS. Delineation of debris-covered ice may be a particular challenge (Glasser et al., 2016; Racoviteanu and Williams, 2012; Scherler et al., 2018).

The Randolph Glacier Inventory compiles these data and sets out guidelines and protocols for data acquisition and analysis. The Global Land Ice from Space (GLIMS) initiative also provides guidelines for the production of these data, and provides an ability to store and compile published datasets (Pfeffer et al., 2014; Racoviteanu et al., 2008; Randolph Glacier Inventory Consortium, 2017; Raup et al., 2007). Most users specify that only glaciers larger than 0.01 km^2 should be mapped due to the challenges in differentiating snow patches and glacier ice for smaller ice masses (Gardent et al., 2014; Paul et al., 2010). These tools allow the compilation of global glacier changes from the 1970s to the present day (e.g., Cook et al., 2014; Kienholz et al., 2015; Malz et al., 2018).

3.2 Topographic maps

Historical topographic maps can provide detailed, high-quality information about glacier extent in the pre-satellite imagery era (Andreassen et al., 2008; Freudiger et al., 2018; Granshaw and Fountain, 2006; Nuth et al., 2013; Tielidze and Wheate, 2018). These maps vary in accuracy, depending on the date of publication and mapping methods used, and so require validation. Data can be visually and quantitatively compared to, for example, locations and correspondence to mountain summits, lakes, valleys, rivers, and independently known glacier extents (Freudiger et al., 2018). These maps can be manually digitized and integrated with assessments of glacier extent from satellite and remotely sensed imagery from later periods. Gardent et al. (2014), for example, used topographic maps, aerial photographs and satellite images to map glaciers in the French Alps in 1967/71 AD, 1985/86, 2003, and 2006/9.

3.3 Historical documents

Historical documents can be used to extend back glacier inventories or records of change to before large scale topographic maps were available. Typically, this will rely on explorers' maps and reports, ship reports, expedition logs and oral histories. This method has the advantage of, unusually, reconstructing glacier advances and maximal extents following Late Holocene neoglaciations such as the 'Little Ice Age'. Normally, evidence for these events is erased from the geomorphological record by the erosive action of glacier ice.

For example, positions of glacier fronts around the Antarctic Peninsula can be identified from aerial photographs, ship logs and maps in the pre-satellite era. These datasets have allowed ice front positions to be reconstructed across the Antarctic Peninsula from the 1940s onwards (Cook et al., 2014, 2005; Ferrigno et al., 2006). These datasets included Antarctic Peninsula maps archived by the British Antarctic Survey, using manuscripts and publications from 1843, maps from 1946-1985, and aerial photographs from 1956-2001 (Ferrigno et al., 2006).

In Patagonia, Chile has numerous historical documents and maps dating from Spanish colonial rule in the 16th Century that have aided the identification of glacier extent over the last few centuries (Araneda et al., 2007). Accounts from early explorers have also provided data on historical glacier positions (Garibotti and Villalba, 2009; Harrison et al., 2007; Izagirre et al., 2018).

In the European Alps, historical drawings, paintings, prints and photographs have enabled the reconstruction of glacier lengths for Mer de Glace (France) and the Lower Grindelwald Glacier, Switzerland, for the last 400 to 500 years (Zumbühl et al., 2008). They were able to reconstruct the advancing glaciers through to 1820 AD, a second maximum extent at 1855 AD, followed by a recession from 1860 to 1880 AD. Likewise, Glacier des Bossons (France) has been reconstructed from 250 pictorial documents (drawings, paintings, prints, photographs, maps) as well as written accounts (Nussbaumer and Zumbühl, 2012). These data allowed the glacier extent to be mapped from AD 1580 with a number of small advances in the 18th and 19th centuries, with the "Little Ice Age" maximum extent reached in 1818 AD. They were also able to show that the glacier is now smaller than at any time in the reconstruction period; an assertion that is challenging to make using other methods.

3.4 Integration of techniques

These archival techniques can be combined with geomorphological mapping and morphostratigraphical approaches to estimate glacier extent from the most recent neoglacial advance (such as the Northern Hemisphere "Little Ice Age"). This provides an ice extent and rates of recession from the 1800s to the present day at a decadal to annual scale (Davies and Glasser, 2012b; Glasser et al., 2011; Meier et al., 2018). In the Swiss Alps, the Siegfried topographic map was published 1878 – 1917 AD (most sheets around 1900 AD), with a second edition from 1917 – 1944 (mostly around 1935 AD). These datasets were compared with glacier extent in 1850 AD (mapped from moraine extent), 1973 (aerial photographs), 2003 and 2010 (satellite imagery) (Freudiger et al., 2018).

3.5 Archival methods quality assurance protocols

High-quality ages derived from historical documents and archives should have a clearly identified textual source, and errors and uncertainties should be discussed. The ice margin should be located in the textual or historical source. Estimates of glacier extent from satellite imagery and aerial photographs should have a measured and specified uncertainty. Estimates of glacier extent from topographic maps must consider the error inherent in map production. All estimates should consider the challenges associated with discerning glacier ice and perennial snow patches. Remotely sensed images should be taken from the end of the ablation season, when minimal snow cover is present. The minimum mapped size of the glacier will be dependent on remotely sensed image resolution and should be considered. DEMs, aerial photographs, satellite images and other datasets must all be correctly geo-referenced for merging into a common dataset (Nuth et al., 2013).

4 Relative chronological methods

4.1 Introduction

Relative dating techniques aim to order landscape features. It assumes that moraines closer to the ice limit are usually assumed to be younger, and those further are older. This is likely to be applicable in temperate environments, but cold-based polar glaciation may override and preserve geomorphological features. Morphostratigraphy is a relative age assignment to surface features (Briner, 2011), based on 'freshness', surface weathering characteristics, or vegetation cover (Lukas, 2006). It has a long history of use, predating the development of numerical dating technologies through the development of relative stratigraphic frameworks (Lüthgens and Böse, 2012). The degree of rock or boulder weathering can be quantified using techniques such as Schmidt Hammer dating, indicating the differential passage of time. Finally, degradation in shells can be measured with amino acid racemization, which may be applicable for older glacial units or where glacial sediments are interbedded with raised beaches (Davies et al., 2009). Relative dating techniques allow practitioners to correlate a small number of landforms with numerical ages to many more landforms over a large spatial area with the same morphometric properties, which is a highly powerful approach to ice mass reconstruction (Briner, 2011), and has been used to interpolate between dated moraines in generating ice-sheet scale reconstructions (e.g. Dalton et al., 2020; Davies et al., 2020).

4.2 Morphostratigraphy

Moraine degradation can be applied as a relative-dating parameter. Moraines are typically deposited with steep sided slopes that degrade with time. The degree of surface roughness and slope steepness is, therefore, a function of moraine age. Measureable features include slope angle, crest width and degree of gullying. Soil thickness, B-horizon thickness and development, and weathering rind thicknesses can be used to indicate relative age (Briner, 2011).

In Scotland, this approach has been used to quantify landforms of Younger Dryas or older age (Boston et al., 2015; Boston and Lukas, 2017; Chandler et al., 2019; Lukas, 2006). Here, the number and type of moraines, number of river terraces inside and outside moraine sequences, the thickness of sediments on sediment-covered slopes, maturity of talus slopes and distribution of periglacial landforms have been used to

differentiate moraines (Lukas, 2006). In the Scottish uplands, 'Type 1' moraines are characterized by small, densely spaced, sharp-crested moraines with intervening meltwater channels and no well-developed river terraces (Boston et al., 2015). These moraines are found in the upper parts of valleys and were assigned to the Younger Dryas. 'Type 2' moraines, in the lower parts of the valley, relate to an older phase of local plateau icefield glaciation or deposition by a larger regional ice mass at the end of the Dimlington Stadial (Greenland Stadial 2; Boston et al., 2015; Lowe et al., 2008). These moraines are characterized by assemblages of large (up to 10 m) sporadically placed moraines with rounded crestlines, surrounded by well-defined river terraces.

These relative chronological methods can be applied to guide a more expensive and time-consuming numerical dating programme (Lüthgens and Böse, 2012). If dating programmes are not based upon a rigorous understanding of sediment-landform assemblages and where relative ages are not well understood, numerical ages can conflict with geomorphological interpretation because samples could have been taken out of context (Boston et al., 2015). Relative morphometric dating techniques such as these can be used to widely correlate moraines across different valleys (Davies et al., 2020), and may provide the only chronological tools where materials suitable for dating are absent (Briner, 2011). However, care should be taken, as topographic controls can result in asynchronous moraine deposition in different valleys (Barr and Lovell, 2014), resulting in glaciers of the same age reaching very different sizes and moraine extents in adjacent valleys (e.g., Davies et al., 2018).

4.3 Schmidt Hammer dating

Schmidt-hammer exposure-age dating assesses the compressive strength of bedrock and boulder surfaces and relates this to the degree of weathering of a surface (Wilson et al., 2019). It is a low-cost relative-dating technique that can be applied rapidly and easily to large numbers of samples in specific locations, allowing for relative ages to be proposed for adjacent features. It has been used in a wide range of Quaternary environments, including glacial landforms (Barr et al., 2017; Shakesby et al., 2006; Winkler, 2014). Schmidt-hammer dating can complement lichenometric dating and guide more expensive cosmogenic nuclide exposure-age dating sampling strategies for boulders on moraines (Wilson et al., 2019).

Schmidt hammers carry out *in situ*, non-destructive tests of material hardness (Goudie, 2006). The hammer measures the distance of rebound of a controlled impact on a rock surface. The 'N' type Schmidt hammer is most frequently used in geomorphological research. It has compressive strength of 20 to 250 MPa. When the Schmidt hammer is pressed against a surface, a piston is automatically released onto the plunger. Part of the impact energy is absorbed by the plastic deformation of the rock and part is transformed into heat and sound. The remaining energy represents the "impact penetration resistance" or hardness of a surface (Goudie, 2006). The distance travelled by the piston after rebound is the "rebound value" (*R*-value). The *R*-value range is 10-100 and is read from a scale on the side of the instrument. Harder rocks have higher *R* values and are by inference less weathered. *R* values, therefore, reflect the structural weakening and chemical breakdown of near-surface rock, and increased surface roughness caused by variable resistance to weathering of surface minerals (Shakesby et al., 2006). This approach can be used to separate moraines formed in different neoglaciations, such as the "Little Ice Age" and older Holocene glaciations (Ffoulkes and Harrison, 2014; Matthews and Owen, 2010; Shakesby et al., 2006; Winkler, 2014) and more recently, even Late Glacial moraines (Barr et al., 2017; Tomkins et al., 2016, 2018a; Wilson et al., 2019) and on blockfields (Marr et al., 2018).

4.3.1 Sampling procedures

R-values should be obtained from horizontal surfaces free from moss and lichen (Shakesby et al., 2006). Samples should avoid the edge of boulders, open and weathered joints, and fissures in the rock. Only stable surfaces should be sampled, and sample surfaces should be dry. The microclimate can impart significant variability, and late-lying snow patches, in particular, should be avoided (Goudie, 2006). Sampling boulders that have surfaces more than 0.5 m above ground level is recommended (Wilson et al., 2019). In any one area, only the same rock types should be sampled, as lithological differences and surface roughness strongly affect *R* values.

In general, multiple measurements should be obtained and the mean value recorded. Practitioners should present the mean value and the 95% confidence interval for each site sampled, separated according to surface type or lithology (Shakesby et al., 2006) (Figure 3). Statistical methods such as Students' T-Test may be used to differentiate between *R* value populations from different sites. Shakesby et al. (2006) found little difference in mean *R* values from particular surfaces in sample sizes of 50, 100, or more readings. This means there may be little advantage in collecting very large samples. Some practitioners discard outliers (Goudie, 2006). Very low values could be due to the rock being weakened by the impact of the hammer, or small rock flaws that were not immediately obvious (Goudie, 2006).

The number of impact measurements taken per boulder varies among practitioners. Ffoulkes and Harrison (2014) used five samples on 40 boulders per moraine, giving a sample size of 200 readings per moraine. Wilson et al. (2019) sampled a single *R* value from 250 boulders per site, using the same operator, the same hammer, and in dry conditions. The hammer was periodically tested against the manufacturers test anvil. The mean *R* value for each site was then calculated. Matthews and Owen (2010) identified 30 sites at each locality for Schmidt-hammer assessment of bedrock. At each site, 25 *R* values were recorded from the bedrock surface. The mean *R* value for the locality was a mean value of the 750 individual measurements. Barr et al. (2017) measured 30 *R* values from three surfaces or boulders on each moraine or site, from numerous horizontal positions on each surface. To assess Schmidt hammer drift during sampling, the same granite boulder was sampled at the beginning and end of the sampling period.

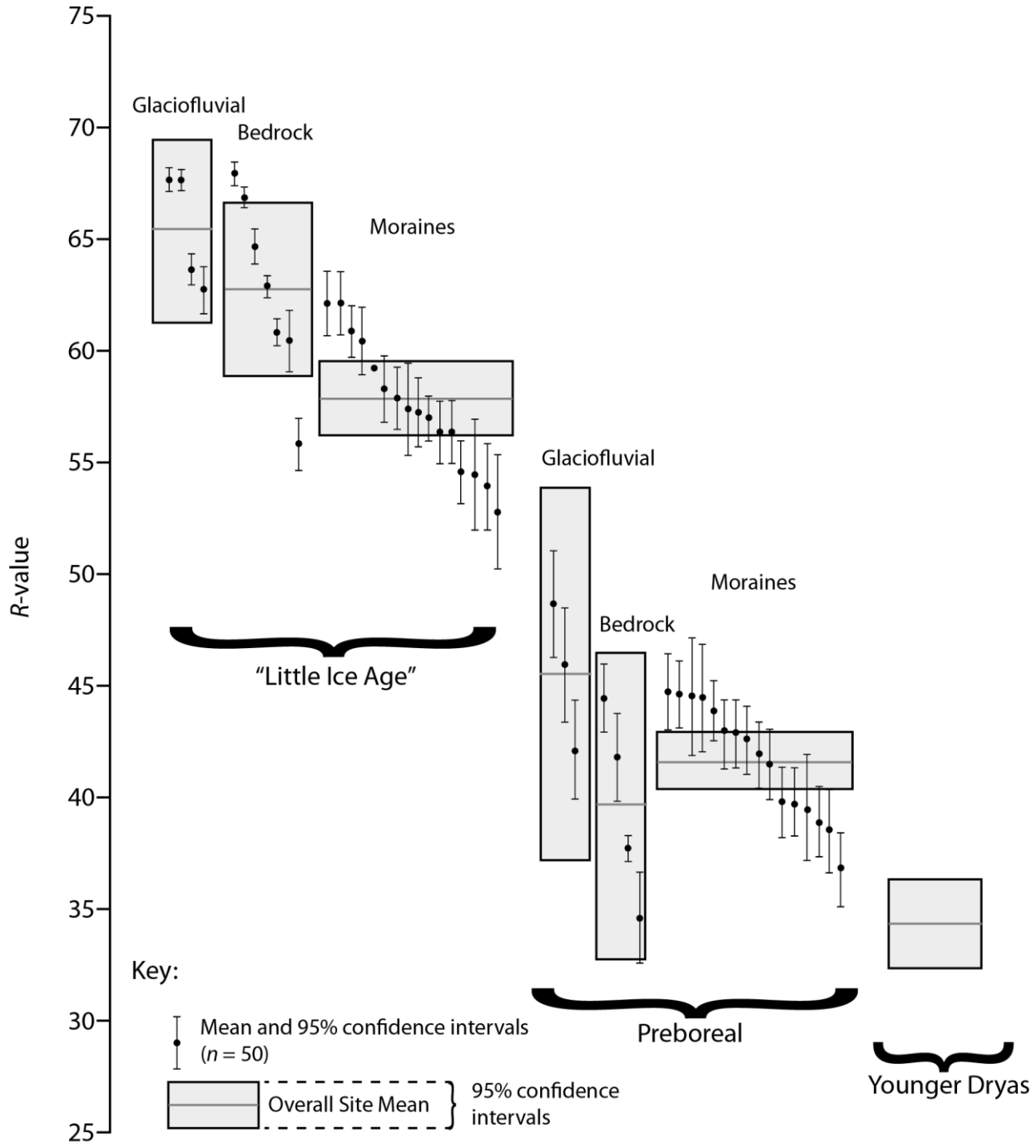

Figure 3. Examples of data presentation, from Shakesby et al. (2006), for Schmidt hammer R-values. Mean R-values with 95% confidence intervals separated according to surface type for sites of 'Little Ice Age' and Preboreal age for the Jotunheimen–Sognefjell and Jostedalsbreen–Sunnmøre sub-regions. The overall means and 95% and 99% confidence intervals are also shown. Redrawn from Quaternary Science Reviews *25(21-22), Shakesby, R., Matthews, J., and Owen, G., pages 2846-2867, title "The Schmidt hammer as a relative-age dating tool and its potential for calibrated age dating in Holocene glaciated environments", Copyright 2006, with permission from Elsevier.*

4.3.2 Calibration and numerical ages

Some operators have attempted to use cosmogenic nuclide ages to calibrate Schmidt hammer *R* values to obtain numerical ages for glacially transported boulders (Tomkins et al., 2018b, 2016; Winkler, 2009). Calibration curves should normally be considered local, and for a specific lithology (Marr et al., 2018; Shakesby et al., 2006). Multiple tie points are needed across the calibration curve, and a regression can then define the *R* value-age relationship. Terrestrial cosmogenic nuclide ages can provide the tie points for linear age-calibration curves and a multiproxy approach to assigning ages to moraines (Wilson et al., 2019; Winkler, 2009). Tomkins et al. (2016) found a statistically significant relationship between 25 granite boulders dated with cosmogenic nuclide dating and Schmidt hammer rebound values, suggesting a linear weathering rate over significant spatial scales for regions of similar climate.

Calculation of numerical ages requires calibration of Schmidt hammer *R* values, against a calibration boulder or independently dated surface (Dortch et al., 2016). However, this approach has been criticized, as it does not differentiate between instrument calibration and conversion of *R* values into numerical age information (Winkler and Matthews, 2016). Tomkins et al. (2018b) provide an online calculator (http://www.shed.earth/shedcalc/) that distinguishes between Schmidt hammer drift following use (instrument calibration) and the development of age calibration curves. They provide an updated age-calibration curve based on 54 independently dating granite boulders (R_2 = 0.94, p = < 0.01) (Tomkins et al., 2018b). The calibration curve dataset extends from 0.8 to 23.8 ka.

4.3.3 Schmidt Hammer quality assurance protocols

Schmidt Hammer data should be collected by a single operator using a single Schmidt Hammer. They should have a clearly defined sampling strategy. Samples should only be compared to those of the same lithology and should be taken from flat surfaces more than 0.5 m above ground level. Schmidt Hammers should be tested and calibrated against the manufacturers' anvil before use, after use to test for drift, and ideally periodically during use. Multiple measurements (>30) should be taken from each surface and a mean value should be computed.

4.4 Amino acid racemization

Amino acid racemization is a chronological tool based on processes of chemical alteration (Penkman et al., 2008). It relies upon the time-dependent breakdown of protein within fossils (Penkman, 2010). Amino acids exist in chemically identical forms, which are non-superimposable mirror images of each other. In living organisms, proteins are almost exclusively made from the left-handed form (L, or 'laeva'). This is unstable, and after death, a spontaneous racemization reaction redresses the balance until there are equal numbers of left-handed and right-handed (D, or 'dextral') amino acids (Penkman, 2010). Over time, the D/L ratio will gradually increase to 1.

In order to interpret amino acid racemization for geochronology, the system must remain closed. In a closed system, the organic material experiences no chemical or physical interaction with the external environment (Penkman et al., 2008). In mollusc shells, amino acids that are susceptible to environmental effects can be removed, isolating the fraction of amino acids that re encapsulated within the mineral crystals of mollusc shells (the intra-crystalline fraction). Amino acid racemization methods can allow terrestrial sequences to be

linked to the deep-sea record of marine isotope stages, and can be applied across Quaternary timescales and into the Late Pliocene (Penkman et al., 2013). Errors are comparatively large, but the method can be used to distinguish between different interglacial and glacial periods (Penkman et al., 2011). Amino-acid racemization progresses at different speeds for different species. By themselves, they do not provide a numerical age estimate, and so the rate of degradation needs to be calibrated for individual sites and species (Lowe and Walker, 2014). For example, the freshwater gastropod *Bithynia* is now well understood, and can provide a comprehensive calibrated dataset for the British Pleistocene (Penkman et al., 2013, 2011).

Amino acid racemization has inherently lower precision, with asymmetric uncertainties, than radiometric methods such as radiocarbon dating, but can be used over a much longer timescale. Where stratigraphic information can be used to constrain thermal history, it can provide useful chronological information (Magee et al., 2009).

Reworked molluscs or bivalves (Demarchi et al., 2012) within older moraines or till sheets or intervening freshwater or marine deposits may be appropriate for this dating technique (Penkman et al., 2010); it can also be applied to raised beaches that may separate glaciogenic sediments from different glacial periods (Davies et al., 2009). Offshore, amino acid racemization can be applied to marine foraminifera with calcareous tests (Kaufman et al., 2013).

5 Incremental methodologies

5.1 Introduction

Incremental dating methods rely on the constant, or incremental, growth or constrained growth rate of an organism (lichenometry, dendrochronology) or incremental sedimentation into a water body (annually laminated lake sediments, or varves) (Lowe and Walker, 2014). The incremental growth may result in annual layering, allowing counting to produce an absolute time scale. If they are missing an identifiable year '0' (i.e., a floating varve or tree-ring chronology that does not extend to the present day), then they must be correlated to a time-anchored chronology or an absolutely dated marker horizon (such as tephrochronology). Annually resolved incremental dating methods have been critical in the calibration of numerical radiometric dating technologies such as radiocarbon dating.

Other incremental dating techniques that are not covered here, as they have less relevance for dating glacial landforms, include annual layers in ice cores, annual increments in speleothems, annual banding in corals and molluscs (Lowe and Walker, 2014), and annual layers in mumiyo (Berg et al., 2019).

5.2 Lichenometry

5.2.1 Assumptions of Lichenometric dating

Lichenometry, mostly using the species *Rhizocarpon* subgenus *Rhizocarpon*, has been widely used to date Late Holocene (last ~1000 years) glacial landforms, including the Northern Hemisphere "Little Ice Age" neoglaciation (Beschel, 1950; Bradwell, 2009; Bull, 2018; Garibotti and Villalba, 2017, 2009; Roberts et al., 2010; Rosenwinkel et al., 2015; Winchester and Harrison, 2000). It has the advantage of being inexpensive and widely applicable. This technique utilises the fact that certain lichen species are slow growing and long-lived, and grow outwards in a radial manner to form crust-like, circular patches on rocks (thalli; McCarthy,

2013). Lichens growing on boulders on moraines will typically be larger with distance from the glacier terminus, meaning that lichen size can be used as a relative measure for the amount of time that glacial debris has been exposed in a stable position, and been available for lichen colonisation and growth (McCarthy, 2013).

Data required to calculate an exposure age, typically of a glacial debris such as a boulder on a moraine, would include growth curve, sampling method, calculated moraine age, and any other relevant information. Lichenometry makes a number of key assumptions (McCarthy, 2013; Osborn et al., 2015):

- A surface can be no older than the oldest individual lichen (thallus) growing upon it;
- Lichen thalli with a circular outline grew radially outwards from a central point;
- The radial growth of lichens is sporadic, but it is constant when averaged over a longer period of time;
- The largest lichen occupies the optimal site for growth, and is the fastest-growing lichen in the vicinity;
- The diameter of the largest or average of the largest lichen thalli with circular outlines can be used to estimate the time elapsed since colonisation began;
- The largest lichen colonised first, and continued to grow through the period between colonisation and observation.

Challenges include variable lichen growth rate due to substrate and microclimatic factors, variable lichen ecesis intervals (the time lag between exposure and colonisation), ambiguous thallus morphology, and potential inheritance of the largest lichens (Osborn et al., 2015). Studies of lichen mortality suggest that the largest lichen may not be representative of exposure age (*ibid*).

5.2.2 Lichenometric species

Species suitable for lichenometric dating have an ecesis time (interval between exposure and colonisation of a surface) of decades to centuries (McCarthy, 2013). Initially, there is a phase of very rapid growth, lasting a few decades, followed by a period of prolonged, steady growth that may last for centuries. Mostly, thalli belonging to the broad group *Rhizocarpon geographicum* agg. are targeted (McCarthy, 2013) (Figure 4). It should be noted that this group includes several aggregated species that may have different growth rates (*ibid*.). However, the challenges of separating these different species in the field means that usually this is in practice ignored.

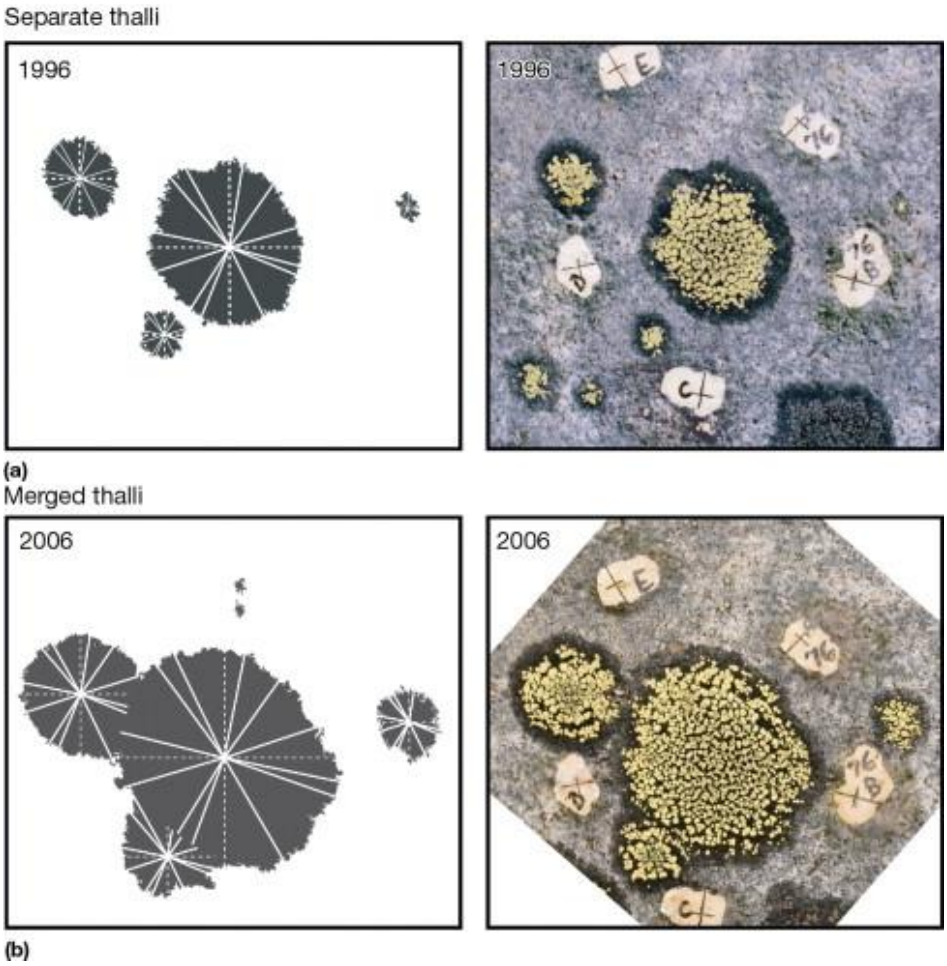

Figure 4. Comparative photographs of Rhizocarpon geographicum agg., *taken ten years apart in 1996 and 2006. The shape and growth of the thalli are not well represented by a single measurement of the diameter; rather, a mean of 12 or more diameters ensures that growth indices are representative. Reprinted from "Encyclopedia of Quaternary Science", McCarthy, D., "Lichenometry", pages 565-572, copyright 2013, with permission from Elsevier.*

5.2.3 Lichenometry sampling strategies

The methods used to collect lichen data are variable among practitioners (Bradwell, 2009). Measurement parameters can include the long axis, short axis, average diameter, largest diameter, modal frequency of lichen sizes and percentage of lichen cover. These variable sampling strategies all have an impact on the construction of lichenometric dating curves. Variations in sampling strategy has led to poor reproducibility among lichenometric studies.

The traditional approach has been to measure the largest lichen (LL) (the diameter of the largest non-competing circular thalli on a surface). Others may measure the mean of the 5 or 10 largest thalli (5LL or 10LL), in order to avoid reliance on a single, and potentially anomalous, sample (Bradwell, 2009). However, the five largest lichens may be statistical outliers and give an anomalously old surface exposure age (Bull, 2018). These lichens may be on reworked boulders with lichen thalli that began growing before their blocks were deposited in a glacial moraine

The fixed-area largest lichen (FALL) restricts the sampling areas (usually boulders) to ~1 m^2. This method assumes that lichen thalli sizes are normally distributed, and that the mean thallus size increases with exposure age (Bradwell, 2009; Bull and Brandon, 1998). This method makes an assumption about the size-frequency distribution of lichens on a surface (Bradwell, 2009) and may be subject to biases imparted by statistical treatment (Osborn et al., 2015).

The Size-Frequency approach (SF) involves the operator measuring the long axis of all thalli of a single species growing within a representative subsample of the surface (25 – 50 m^2). Sample sizes of >1000 thalli are recommended (Benedict, 2009; Bradwell et al., 2006). This method measures and quantifies the size-frequency distribution of a lichen population.

The lichen cover approach (LC) assumes that the percentage of a rock covered with a single species of lichen will increase with time. This technique is more subjective and involves estimating the percentage of lichen cover, so it is only recommended when other approaches are impractical (Bradwell, 2009).

A number of papers review these different techniques, and make different recommendations (Bradwell, 2009; Bull, 2018; McCarthy, 2013; Osborn et al., 2015). Bull (2018) recommends that accurate dating of surface exposure times using lichenometry should use measures of central tendency, by obtaining large datasets of the largest lichen thallus diameter (LL) on many blocks or boulders. Users should plot histograms of the largest lichen diameter (LL) and use the histogram peaks to determine the mean largest lichen size and thus the relative (and absolute if calibrated) age of the moraine (Bull, 2018).

5.2.4 Calibration curves of lichen growth rate

Lichen growth rates are spatially and temporally variable, making it challenging to construct a growth curve. Firstly, growth rates are susceptible to climatic variability. In Patagonia, for example, the strong east-west precipitation gradient introduces statistically significant differences in the growth curves (Garibotti and Villalba, 2009). This means that the site-specific calibration of lichen growth rates is required.

Secondly, lichen thalli begin growth after an ecesis time (the lag interval between exposure and colonisation) that varies between a decade or longer than a century (McCarthy, 2013), and which is frequently poorly constrained (Evans et al., 1999).

Thirdly, the growth rate of *Rhizocarpon* decreases over time. Growth is initially rapid, which lasts for several decades, followed by steady, linear growth that can last centuries. This makes it unfeasible to simply extrapolate growth rates from a small number of control points. In addition, there are some challenges for dating longer exposure ages, as the loss of the central part of a thallus due to weathering is common in older samples, and recolonization can make it challenging to distinguish individual thalli (*ibid*.).

Growth curves require, as a minimum, indices of thalli size in a known calendar year (McCarthy, 2013). However, the development of lichen growth curves remains problematic. True growth curves should involve the repeated observation of the areal growth in a marked individual thallus over time, rather than the more usual thallus size-surface age scatter plots (Osborn et al., 2015).

5.2.5 Lichenometry quality assurance protocols

Deriving exposure ages from lichenometry remains challenging, and a number of studies may not be reproducible due to the variable methodologies employed and the assumptions made. Each sampling

methodology has weaknesses, and the lack of standards and no definitive useful temporal range is very concerning (Osborn et al., 2015). Development of sampling protocols remains challenging. Practitioners are recommended to carefully review their assumptions and sampling methodologies. Crustose lichens remain useful as relative-age indicators, and large *R. geographicum* thalli may indicate that a moraine pre-dates the "Little Ice Age", but a method for delimiting a growth curve to determine absolute ages remains challenging (Osborn et al., 2015).

5.3 Dendroglaciology

5.3.1 Introduction to Dendroglaciology

Trees colonising recently deglaciated land surfaces, especially on markers of ice advance such as moraines, provide a means of dating surfaces that are too young to date reliably by other means (Coulthard and Smith, 2013; Koch, 2009; Smith and Laroque, 1996). This has been termed 'dendroglaciology' (Masiokas et al., 2009). By using long-established tree-ring dating principles (Douglass, 1914; Shroder Jr, 1980), it is possible to assign ages to landforms and landscape processes. Commonly, this involves dating trees killed directly or indirectly by a glacial advance, and possibly being reworked into moraines, establishing the age of trees growing directly on glacial landforms, or dating growth irregularities in ice-marginal trees affected by glaciers (Figure 5) (Coulthard and Smith, 2013), such as tilting or scars. This method works well in temperate regions where glaciers extend down into well-forested areas during the Late Holocene, such as New Zealand, North America and Patagonia, and operates over a scale of centuries (Barclay et al., 2009; Wiles et al., 1999).

5.3.2 Glacially killed trees

Glaciers may kill trees by expanding into forests, shearing tree trunks, burying trees beneath glacial sediment, or partially burying them in outwash sediments (Figure 5) (Barclay et al., 2009; Jackson et al., 2008; Koehler and Smith, 2011). Tree stumps may be protected in downstream low-pressure zones and downstream of bedrock protrusions (Coulthard and Smith, 2013). If the tree stump remains in a growth position, the kill date indicates the glacier position at a specific time. This requires a tree-ring master chronology to determine the tree age (*ibid.*).

Alternatively, mats of organic woody material may be reworked into moraines (Coulthard et al., 2013), where they can be radiocarbon dated (Koehler and Smith, 2011), or if they are sufficiently well preserved, provide floating chronologies that can be related to existing 'master' tree-ring chronologies (Wiles et al., 2011). The dating potential and precision is dependent on preservation, especially of the outer rings and bark. For example, at Icy Bay in southern Alaska, USA, subfossil logs were found in growth position; other logs were reworked into till. These logs were radiocarbon dated to find the timing of glacier advance (Barclay et al., 2006). Tree-ring samples were collected from each log, and samples were analysed to determine the preservation of the last years of growth. Cross-dating was attempted for spruce and hemlock logs with >65 rings. Samples were initially cross-dated with other subfossil logs, and then compared with a master chronology from Sitka spruce growing on nearby glacial outwash. Together, these data extended the glacial history of Icy Bay back to 3800 years ago, and revealed a number of advance-retreat cycles (Barclay et al., 2006).

Koehler and Smith (2011) used dendroglaciological and lichenometric methods to develop a perspective of glacier fluctuations over the last 5000 years in the British Columbia Coast Mountains, Canada. Their data showed that glaciers had periodically extended below the treeline over this time period, overriding and burying forests beneath tills. Subfossil specimen were related by tree-ring cross dating to a new master chronology, developed on adjacent mature subalpine fir trees (Koehler and Smith, 2011). Radiocarbon ages from perimeter weed samples helped constrain the timing of tree death and anchor floating chronologies. These data showed glacier expansions at 4.76 and 3.78 ka, and then glacier recession allowed regrowth of trees (>200 years) by 2.42 ka. A substantial glacier advance occurred after 2.42 ka and again during the "Little Ice Age" in the 19th and 20th centuries.

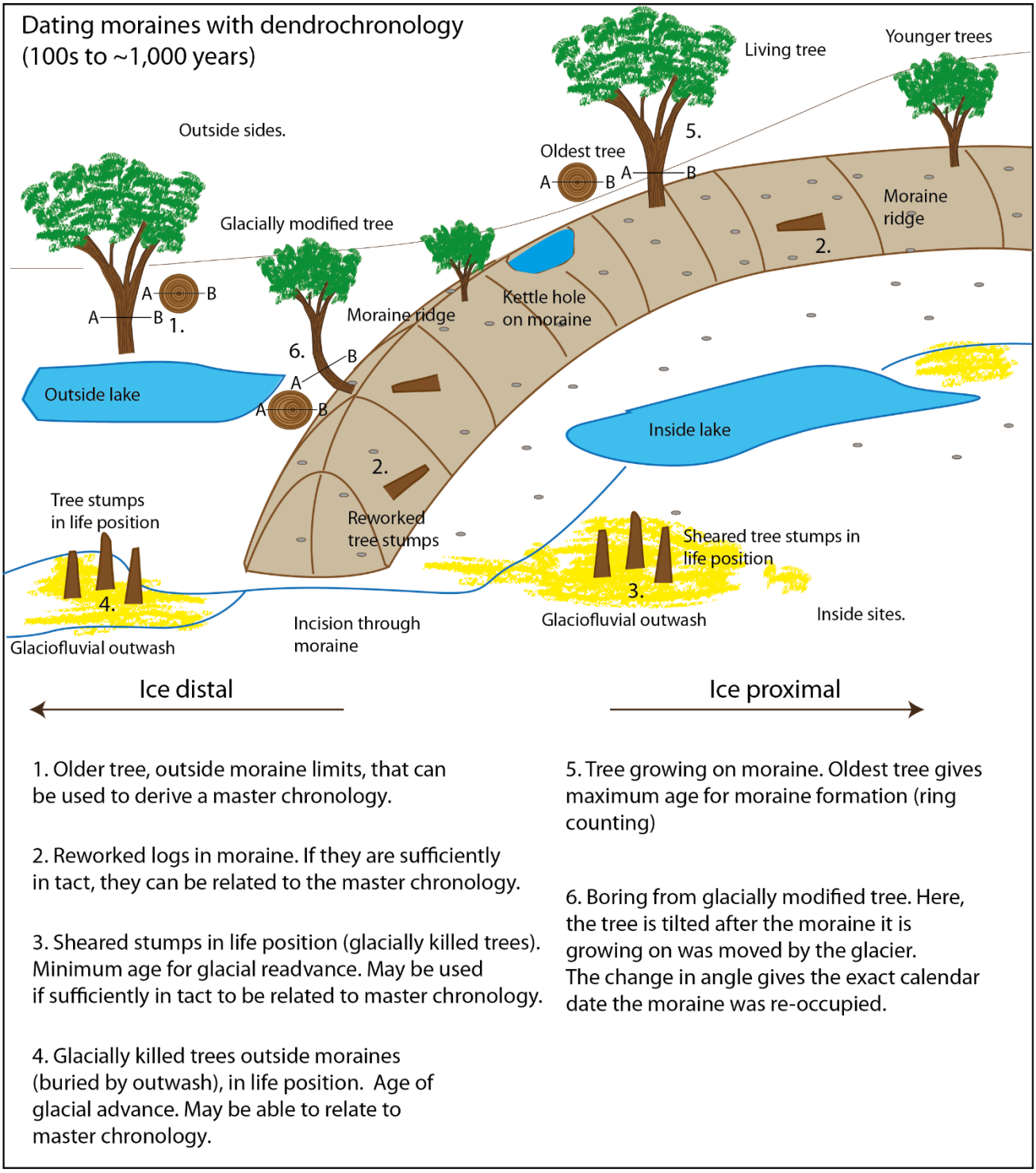

Figure 5. Cartoon illustrating examples of how tree-ring dating can be used to date moraine formation.

5.3.3 Glacially damaged trees

Glacier advances may scar or cause growth irregularities in ice-marginal trees. Glacial landforms or ice-marginal trees may be shunted, tilted or otherwise moved by glacier fluctuations. Trees that are tilted may continue to grow, and the irregularity in their annual rings can be dated. Trees may also be scarred by

surface abrasion from glacier advances, and the date of this scar can be calculated from the development of callous tissue on tree stems (Coulthard and Smith, 2013).

5.3.4 Surface dating

Assessing the age of trees growing on glacial landforms, such as terminal or lateral moraines, can provide a minimum exposure age for the moraine (Wiles et al., 1999). This method has a dating precision of around 10 years, and the age of the oldest tree provides a minimum estimate for the surface age (Coulthard and Smith, 2013). Limitations of the technique include that the ecesis time (time between surface exposure and tree germination) is challenging to estimate (Koch, 2009), and it makes the assumption that the oldest tree has been sampled. It is therefore recommended to sample a number of trees at a site, particularly if the site is well forested and the oldest tree difficult to locate (Coulthard and Smith, 2013).

This surface-dating application of dendroglaciology works well on glacial landforms that date from the last few centuries. For example, it has been widely applied to date "Little Ice Age" moraines around the North Patagonian Icefield and South Patagonian Icefield (e.g. Boninsegna et al., 2009; Koch and Kilian, 2005; Masiokas et al., 2009; Warren et al., 2001; Winchester et al., 2014, 2001; Winchester and Harrison, 2000). Here, most tree-ring chronologies use the South American beech (*Nothofagus* sp.), the conifer *Pilgerodendron uviferum* or *Fitzroya cupressoides*.

5.3.5 Dendrochronology quality assurance protocols

High-quality moraine ages from dendrochronology would have an ecesis time and growth rate that has been calculated and provided, a clear sample context, and the age of the tree should be clearly calculated.

5.4 Varve records

5.4.1 Introduction to varve chronologies

Ice-dammed or proglacial lakes can provide a means of dating ice-marginal fluctuations through the analysis of annually laminated (varved) sediment sequences (Bendle et al., 2017; Caldenius, 1932; Larsen et al., 2012; Palmer et al., 2010; Ridge et al., 2012). Some lacustrine records extend back to before the Last Glacial Maximum (Zolitschka et al., 2015). Varves can be clastic (detrital), biogenic or endogenic. Clastic varves form when a lake receives siliciclastic particles through alluvial activity, slope wash or aeolian sources (Zolitschka et al., 2015). Biogenic sedimentation results from biological production of organic matter and biomineralisation in the water column. After death, the organisms may be remineralised or metabolically oxidised. Endogenic (mineraogenic) sediments receive crystallising particulate matter via chemical precipitation of minerals from the water column (Zolitschka et al., 2015). In proglacial lakes, clastic varves form in response to seasonal variations in sediment influx that lead to deposition of a coarse-grained (silt/sand) melt season layer, capped by a fine-grained (clay) non-melt season layer.

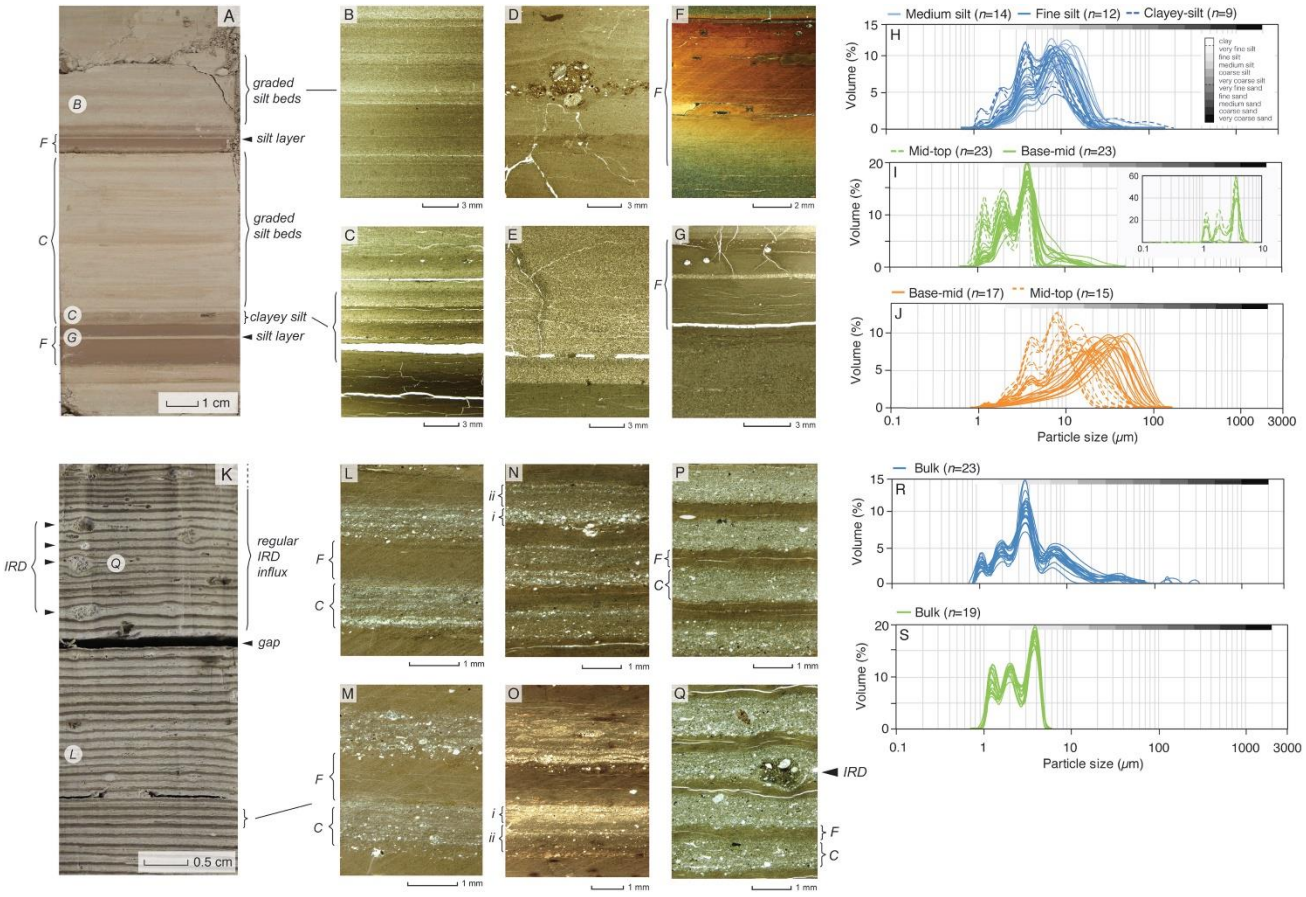

Figure 6. From Bendle et al. (2017). *Examples of typical varve macro and micro-facies within >cm scale varves (A-G) and <cm scale varves (K-Q), along with supporting particle size information (H-J and R-S). For more information, the reader is referred to Bendle et al. (2017).*

5.4.2 Varve counts

Where deposited in continuous sequences, counts of the number of annual layers enable an incremental chronology to be developed. This can give a period of time when the glacial lake was in existence. Varve counts must have careful criteria to note each varve (Zolitschka et al., 2015), and may require micromorphological analysis of thin sections in order to provide robust counts of microscopic varves (Ojala et al., 2012; Palmer et al., 2012). Operators must document carefully how varves were identified and counted in order to ensure accuracy. The accuracy is dependent on the structure, composition and distinctiveness of the varves, which must be carefully described and reported, and estimates of varve-counting error should be provided. The best varve chronologies typically have an accuracy of ± 1 to 4% (Ojala et al., 2012).

There are two principle methods used to count and record varves. Firstly, where varves are distinctive and thicker than ~0.5 mm, freshly cleaned measured sections can be directly counted in the field or from core halves. Photographs can be used to record varves (Ojala et al., 2012). It works best when there are frequent distinctive marker beds. This technique requires high-resolution photographs and very detailed sedimentological descriptions, and core-to-core correlations must be very careful.

Alternatively, sediments can be embedded in epoxy resin, polished and mounted as thin sections. Microscopic analysis and image analysis techniques can document and count the varves (Bendle et al.,

2015). Non-destructive and rapid scanning technologies, such as X-Ray microtomography, allow material samples to be analysed in three dimensions. Together, these methods allow for a very high-resolution analysis of the sequences.

Before glacier fluctuations can be dated, this 'floating' varve chronology must be anchored in absolute time using an independent dating technique such as tephrochronology (e.g., MacLeod et al., 2015) or radiocarbon dating. However, biological productivity is supressed in cold periods, and glaciolacustrine varves are often biologically barren, making radiocarbon dating challenging (Devine and Palmer, 2017). In places with on-going sedimentation, the top-most varve can be taken as the year of coring (year 1), providing an anchor point (Zolitschka et al., 2015).

Once time-anchored, a varve record can be used to infer glacier changes (often using a combination of varve thickness data and the morphostratigraphic relationship between varved sediment sequences and ice-marginal landforms, such as moraines) and date their timing. As an example, a sequence of varves deposited between two recessional moraines enables age estimates to be derived for each of these former glacier extents. Using this approach, the duration of glacier retreat cycles and rates of recession can be quantified (e.g., Bendle et al., 2017).

5.4.3 Varve thickness

Varve thickness in a glaciolacustrine environment is controlled by sediment flux into a lake during the summer melt season (Devine and Palmer, 2017), and by limnological factors that affect the transportation of this sediment during the year. Varve thickness is useful, because it can be related to climate (Bendle et al., 2019), the extent to which the catchment is inundated with glacial ice, and the proximity of the ice margin. Distal varve chronologies, located far from the ice margin in ice-dammed palaeolakes, are advantageous for constructing chronologies of glacial extent because they are less susceptible to processes that disrupt sedimentation (Devine and Palmer, 2017). Distal locations are, therefore, more likely to preserve longer, continuous records.

In Patagonia, glaciolacustrine varve records were first studied by Caldenius (1932). However, in this early work, the absolute timing of glacial changes could not be ascertained as no means of independent dating was readily available. Recently, however, a varve chronology of *ca.* 1000 years duration was developed at Lago General Carrera-Buenos Aires. This record has been independently dated through tephrochronology, owing to the *in situ* presence of the Ho tephra (Table 1) in the varve sequence (Bendle et al., 2017). These ages complement ^{10}Be dating of moraine boulders in the same valley (Douglass et al., 2006; Kaplan et al., 2004; Thorndycraft et al., 2019).

5.4.4 Varve count quality assurance protocols

High-quality varve ages should include a process model of varve formation, and multiple varve counts should be carried out by independent experts. The varve count uncertainty should be expressed. A 'floating' varve chronology should be anchored in time using tephrochronology or radiocarbon dating. Where stratigraphic context is clear, varve years can provide an age for a moraine with a measured uncertainty. This can be independently checked with bracketing tephra, radiocarbon or optically stimulated luminescence ages inside and outside the ice margin, or cosmogenic nuclide ages from the moraine.

6 Age equivalent stratigraphic markers

6.1 Introduction

Age-equivalent stratigraphic marker horizons are those distinctive horizons with a uniform age. They are broadly synchronous and form time planes across different sedimentary sequences. The horizons must be independently dated by radiometric or incremental methods, and then can allow age estimates to be extended to other sequences with the marker horizon (Lowe and Walker, 2014). They are an indirect means of dating, but because of their widespread distribution, can be essential for understanding and creating stratigraphic correlations between sites.

Tephrochronology, the use of volcanic ash layers as a means of dating, is widely applicable across Quaternary timescales and allows precise correlations and tie-points between sites. It is particularly useful when radiocarbon dating is unfeasible or problematic, such as in calibration plateaus. Palaeomagnetism is the identification of the polarity of rocks and sediments, which allows them to be assigned to a particular magnetic epoch. Biostratigraphy is the use of palaeoecological or evolutionary events to provide a correlation between older Quaternary deposits. These tools are useful for assigning older deposits to certain marine isotope stages.

6.2 Tephrochronology

“Tephra” refers to the explosively erupted, loose, fragmental material erupted in volcanic eruptions (Alloway et al., 2013). It includes all grain sizes from fine dust to boulders. Tephra deposits are erupted and deposited over short time periods, and they can be spread widely over land and sea as a thin layer that has the same age in all localities. Tephra horizons can be related to specific and independently dated eruptions by fingerprinting their mineralogical or geochemical properties. As such, a tephra layer, once identified, provides a time-parallel marker isochron for a specific point in time (Alloway et al., 2013). Tephrochronology has an advantage in glacigenic sediments such as barren glaciolacustrine varves, where radiocarbon dating is unfeasible.

“Tephrochronology” is the use of these tephra horizons to link stratigraphies in different settings via these precise tie points. It is increasingly used as a global dating tool across the world, in terrestrial (MacLeod et al., 2015; Monteath et al., 2019) and marine environments (Abbott et al., 2018; Di Roberto et al., 2019) and ice cores (Abbott et al., 2016; Cook et al., 2018). Tephrochronology relies upon the identification of a tephra layer and its correlation to deposits elsewhere, and ideally to a particular eruption event. The identification relies upon physical, mineralogical and geochemical properties, together with stratigraphic and age relationships (Lane et al., 2017; Lowe, 2011).

The value of tephra horizons as a geochronological unit lies in its ability to act as both dated age markers (tephrochronology), and event-stratigraphic horizons (tephrostratigraphy). This allows the correlation of different sedimentary or volcanic archives. Tephrochronology spans a longer period than many other chronological techniques, and has no theoretical upper limit provided that the geochemical and taphonomical integrity of the sample can be demonstrated (Lane et al., 2017).

Tephra thus allows the synchronisation and dating of high resolution palaeoclimate records, and the transfer of ages from one site to the next (Lowe, 2011). A number of international collaborative efforts such as INTIMATE (Integration of ice core, marine and terrestrial records: refining the record of the last glacial-

interglacial termination) and RESET (Response of humans to abrupt environment transitions) rely on tephrochronology to underpin high resolution records (Blockley et al., 2014; Davies et al., 2012; Lowe et al., 2008; Ramsey et al., 2015; Rasmussen et al., 2014).

6.2.1 Cryptotephra

The ability of fine-grained tephra shards to be dispersed over very large distances allows broader time-synchronous marker horizons to be identified. These "cryptotephras" are not visible as a layer in the field, but can be identified through careful and systematic microscopic examination of sediment cores (Davies, 2015). Cryptotephras can be found in peatlands, lakes, ice and marine cores (Abbott et al., 2018, 2016), allowing stratigraphic sequences to be correlated across different depositional environments, and providing tie points for climate reconstructions (Watson et al., 2016).

Geochemical analysis of single shards allows fingerprinting for the successful correlation of deposits. These sparse deposits can thus be traced and correlated over great distances. This requires the establishment of regional tephrochronological frameworks that include well-dated age estimates and a robust chemical signature for each deposit (Davies, 2015). An example is the Vedde Ash, an Icelandic cryptotephra that has been mapped in western Russia, Switzerland, Slovenia, northern Italy and the UK.

Secure chemical identification and robust dating of individual tephra layers is challenging, due to the difficulty in differentiating individual tephra layers that originate from volcanic sources with very similar chemical signatures (Timms et al., 2019). There are also challenges associated with distinguishing primary fall deposits from reworked material, and the need for universally standardised procedures for the chemical fingerprinting of tephra materials.

These challenges require that tephrochronologists develop regional stratigraphic frameworks that integrate the stratigraphic, chemical and chronological information for all tephra layers within certain time intervals (Fontijn et al., 2016; Lowe et al., 2015; Timms et al., 2019). This approach identifies the tephra layers that best serve as reliable isochrons, and the geographical 'footprints' over which they are observed.

A challenge with cryptotephras is that identification is strongly related to taphonomy. The microscopic glass shards are prone to reworking or chemical alteration. Peatlands capture a smaller volume of tephra shards, as they capture only primary tephra fall. Lakes can concentrate tephra horizons, as tephra falling across their catchment subsequently washes into the lake (Watson et al., 2016).

Tephrochronology can be used to date (glacio)marine sediment cores, complementing radiocarbon chronologies, and allowing correlation between terrestrial and marine sequences (Matthews et al., 2015). The independent dating control provided by tephrochronology can be especially valuable where the radiocarbon marine reservoir effect is poorly constrained. However, reworking processes, including *in situ* bioturbation and sediments being eroded, re-suspended and redeposited by ocean currents can make resolving sequences into discrete volcanic eruption events challenging (Matthews et al., 2015).

6.2.2 Dating tephra horizons

Before tephra horizons can be used most effectively for stratigraphic chronologies, they must be independently dated (Alloway et al., 2013). They can be dated by historical and eyewitness accounts of tephra falls or eruptions, fission-track dating, Ar/Ar dating, and dating enveloping or entrained materials by

radiocarbon dating, luminescence dating or other means. Historical accounts are most common over the last 200 to 300 years, but in some places oral and written accounts of eruptions date back much earlier. Tephra ages are chronologically constrained using ^{14}C dates from terrestrial sites, and are thus independent of marine reservoir corrections (Kilian et al., 2013).

6.2.3 Application of tephrochronology to glacial landforms

Tephrochronology of layers in sediment cores can provide an improved chronostratigraphy. This geochronological tool is applied where archives of sediment can be related to glacial landforms; this could include varved lake sediments dammed by a moraine, or sediment cores extracted from kettle holes or lakes associated with glacial retreat. Where these studies are done in conjunction with repeated radiocarbon ages and subsequent tephra horizons, they provide an excellent independent marker horizon of a known age across several cores. In the absence of dateable organics at the base of sediment cores, tephra horizons can provide a constraint on the timing of deglaciation, correlated across multiple cores and localities (e.g., Kilian et al., 2013, 2007, 2003; Stern, 2008).

As an example, in Patagonia, six key volcanoes (Lautero, Viedma, Aguilera, Reclus, Mt. Burney and Cook Island) form the Andean Austral Volcanic Zone, which is the southernmost volcanically active segment in the Andes (Stern, 2008). Hudson volcano is important further north (Bendle et al., 2017). These volcanoes result from slow subduction of the Antarctic Plate. These volcanoes deposited regionally widespread Holocene tephra layers in Tierra del Fuego, which can be geochemically distinguished. The key tephras from this region are summarised in Table 1.

The presence of tephras in oceanic or lake sediments or bog mires can date ice-free conditions and help ascertain the timing of glacier recession. The large number of well-identified tephras across the Late Glacial and Holocene in Patagonia (Table 1) enables clear reconstructions (Kilian et al., 2003; Sagredo et al., 2011; Stern, 2008; Stern et al., 2016; Weller et al., 2015). For example, the identification and correlation of tephras within sediment cores obtained from stratigraphically meaningful sites helped constrain the rate and manner of deglaciation of the Última Esperanza Lobe in Patagonia during the Late Glacial period (Sagredo et al., 2011).

Table 1. Details of key Holocene tephra layers distributed in southernmost South America.

Source	Tephra	Latitude	Average ^{14}C yrs BP	Average cal. yrs BP	Reference
Reclus	R_1	51°S	12,685 ± 260	14780 ± 560	Sagredo et al. (2011)
Mt Burney	MB_1	52°S	8440 ± 750	9400 ± 1100	Stern (2008)
Mt Burney	MB_2	52°S	4015 ± 720	4265 ± 895	Stern (2008)
Hudson	Ho	45°S	18820	17370 ± 70	Stern et al. (2015); Weller et al. (2015)
Hudson	H_1	45°S	6850 ± 160	7710 ± 280	Stern (2008)
Hudson	H_2	45°S		4000 ± 50	Stern et al. (2016); Naranjo and Stern (1998)

Hudson	H_3	45°S		1991 AD	Stern et al. (2016)
Aguilera	A_1	50°S	3000 ± 100	3200 ± 270	Stern (2008)
Mentolat	MEN_1	44°S	6782 ± 23	7490 ± 130	Stern et al. (2016)

In Iceland, the proximal location of volcanoes and glaciers means that tephrochronology is well established (Kirkbride and Dugmore, 2008, 2003). Two glaciers and Eyjafjallajökull, south Iceland, underwent multiple episodes of glacier advance over the last two millennia, with moraines dated through tephrochronology and lichenometry (Kirkbride and Dugmore, 2008). Detailed maps showed moraines and ice-marginal glaciofluvial and glaciolacustrine landforms. Tephrostratigraphy from sites in between moraines and associated outwash deposits allowed bracketing numerical ages to be assigned to moraines. These tephra layers, identified and correlated on the basis of geochemical fingerprinting, allowed the formation of isochrones defined by the base of a tephra layer. Where soil drapes over a moraine, the basal tephra in the soil profile gives a minimum age for the glacial advance (Kirkbride and Dugmore, 2008). In forefields, the first tephra above a recessional till provides a minimum age for ice recession.

Across the UK, the majority of the individual cryptotephra layers have been traced to volcanoes in Iceland; this is due to the generally westerly storm track in the North Atlantic. In Scotland, traces of non-visible volcanic glass shards (cryptotephra) were found in sediment cores taken from Kingshouse, western Rannoch Moor, to constrain the timing of ice disappearance (Lowe et al., 2019). These data indicated that glaciers in this area continued to expand until the end of the Younger Dryas period. Here, detailed analysis of varves that formed in the Roy-Spean ice-dammed glacial lakes, anchored in time through detailed tephrostratigraphical studies, indicated that ice lobes were still advancing after ~12.1 ka BP, and persisted as major barriers that held back major ice-dammed lakes until ~11.6 ka BP (Lowe et al., 2019).

6.2.4 Tephrochronology quality assurance protocols

High quality tephra ages would be consistent and in stratigraphic order with other tephra layers and ideally with independent radiocarbon dating. The tephra should be geochemically analysed and compared with other tephras. The tephra layer should be independently dated with robust uncertainties.

6.3 Palaeomagnetism

Palaeomagnetism is a relative dating tool that can be applicable for dating moraines or sediments that predate the last glacial cycle. Palaeomagnetism is based on changes in the Earth's magnetic field as is preserved in rocks and sediments. The Earth's magnetic field is *dipolar*; it possesses two poles (north and south). Over time, the magnetic field changes in direction and field strength (Lowe and Walker, 2014). In major dipole changes, the dipole field is reversed and the magnetic North and South Pole flip. These polarity changes are measured over thousands to millions of years. Sedimentary environments preserve these magnetic changes. Magnetic minerals will form a natural remnant magnetism, a reflection of the geomagnetic field at the time of deposition. See Lowe and Walker (2014) for reviews.

Polarity reversals can be detected in the geological record. The present-day magnetic field has a normal polarity; the opposite is a reversed polarity. Periods with long-term fixed polarity are termed 'polarity

epochs'. Two polarity epoch boundaries are recognised in the Quaternary; the Bruhnes-Matuyama (K-Ar dated to c. 0.73 Ma), and the Matuyama-Gauss (K-Ar dated to 2.47 Ma) (Lowe and Walker, 2014). The Gauss-Gilbert chron is K-Ar dated to 3.41 Ma (Figure 7). In addition, there are shorter-term polarity reversals of shorter duration, termed 'polarity events'. Important Quaternary polarity events include the Jaramillo 'normal' event (K-Ar age of 0.90 to 0.97 Ma) and the Olduvai 'normal' event (K-Ar age of 1.67 to 1.87 Ma) (Lowe and Walker, 2014) (Figure 7). This method can be useful for identifying moraines that were deposited in the Early to Mid-Pleistocene.

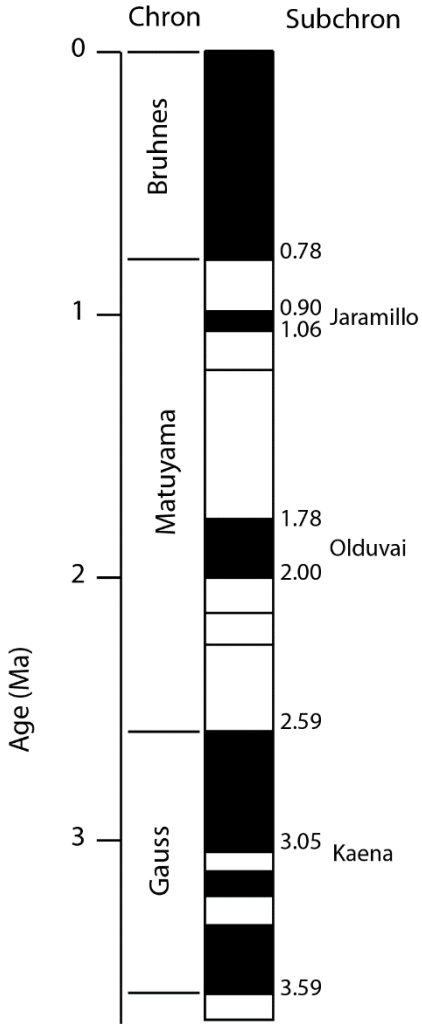

Figure 7. Palaeomagnetic Chrons and Subchrons. Black indicates normal polarity and white is revered polarity.

Palaeomagnetism in moraines allows different glacial drifts and moraines to be assigned to different time periods. In the Rio Pico valley in Patagonia, a series of four nested moraine sets all show normal polarity magnetisation and correspond to the Bruhnes Palaeomagnetic Chron (Rabassa et al., 2011). In the Lago Buenos Aires region of Patagonia, palaeomagnetism showed that the two inner of five sets of moraines had a normal (Bruhnes) polarity, whilst the outer two zones had a reversed (Matuyama) polarity (Mörner and Sylwan, 1989). In the Mackenzie Mountains, Canada, palaeomagnetism revealed a series of interbedded glacial sediments and palaeosols, indicating a long record of glacial and interglacial cycles. The oldest

sediments had a normal (Gauss) polarity, and were overlain by reversed (Matuyama) polarity and then normal (Bruhnes) polarity sediments (Duk-Rodkin et al., 1996).

In Kenya, moraines marking an Early Pleistocene glaciation, interbedded with loess and palaeosols. These sediments, assigned to the Gorges Glaciation, rest on weathered tuff with Gaussian polarity. The lower till body (Pre-Gorges Glaciation) is reversely magnetised, suggesting it belongs to the Matuyama Reversed Chron, and has an overprint record that is likely pre-Olduvai in age (Mahaney et al., 2013). Gorges ice advanced into the region during the Olduvai Chron (1.78 – 2.0 Ma), truncating the buried profiles. Overlying palaeosols have a reversed overprint, denoting their placement within the Late Matuyama. Surface soils have a magnetic polarity accordant with the Bruhnes Chon (Mahaney et al., 2013).

6.4 Biostratigraphy

Biostratigraphy is the application of fossil data as an age-equivalent stratigraphic marker. This can provide direct or bracketing ages for glacial sediments. This can include vegetation changes, since regional pollen assemblage zones will be effectively time-parallel (Lowe and Walker, 2014; Roe et al., 2009), which can be used for correlation, especially in the Holocene. Likewise, mammalian fauna have varied between interglacials in many countries. Faunal turnover was high during the Quaternary because extinctions, immigrations and evolutionary changes were forced by large-scale climatic events (Schreve, 2013). If these mammal assemblage zones can be identified and characterised, they can also be used as age-equivalent stratigraphic markers (Schreve, 2013, 2001). These data can be linked to large-scale river terrace systems (Bridgland, 2000; Bridgland et al., 2001; Rose, 2010; Schreve, 2009) and glacial deposits that predate the last glaciation (e.g. White et al., 2017). This technique has been used in North Norfolk, UK, prompting a large-scale debate regarding the age of Middle Pleistocene glacial and interglacial sediments (Gibbard and Clark, 2011; Lee et al., 2011, 2004; Preece et al., 2009).

Mammalian evolutionary changes in the Quaternary can also be applied as age-equivalent stratigraphic markers. Of significance in Europe is the lineage of the large water vole, *Arvicola terrestris cantiana* (Lowe and Walker, 2014), which evolved from the earlier species of vole, *Minonys savini* (which had in contrast rooted molars) during the Cromerian, and after the Bruhnes-Matuyama palaeomagnetic boundary (~MIS 19). These fossils have been used to constrain the age of Middle Pleistocene glacial sediments in north Norfolk, UK (Preece et al., 2009).

7 Summary and conclusions

Glacial landforms such as moraines provide a distinctive point in time demarcating a glacier's extent. Trimlines or lateral moraines can denote glacier thickness. These substantial depositional landforms form when a glacier is in equilibrium with the climate, and remains at a certain point long enough to build distinctive ice-marginal features such as moraines. Independent dating of these features is required in order to constrain the timing of these advances and stabilisations, and rates of glacier thinning and retreat. Quantifying past rates and magnitudes of change and being able to link these to independent proxies for palaeoclimate allows researchers to constrain the climatic and internal drivers of past ice-mass variability. Using these datasets in conjunction with numerical simulations of ice flow and mass balance, forced by independent climatic proxy data, helps researchers understand glacier-climate relationships, and to predict the future evolution of these ice masses.

This chapter has summarised some of the key concepts required for consideration when attempting to date glacial environments, including the concepts of absolute and relative dating techniques, direct and indirect dating techniques, the length of time for different chronometers, precision and accuracy, and minimum and maximum ages. This chapter covered the principles, protocols, sampling methodologies and quality assurance protocols for archival dating methods (remote sensing using aerial photographs and satellite imagery, topographic maps, historical documents), relative chronological methods (morphostratigraphy, Schmidt Hammer, Amino Acid Racemization), incremental methods (lichenometry, dendroglaciology, varve records) and age-equivalent stratigraphic markers (tephrochronology, palaeomagnetism, biostratigraphy), and their specific application to dating glacial landforms. In conjunction with radiometric dating techniques (such as radiocarbon dating, cosmogenic nuclide dating, optically stimulated dating, potassium-argon and argon-argon dating), these techniques can be used in a wide range of different environments and across different timescales to accurately reconstruct past ice-mass dynamics. Different methods may be applied together to produce the best outcomes for dating glacial landforms and reconstructing palaeoglaciers.

Each method has its own limitations and must be applied within the relevant geomorphological and sedimentological frameworks. This ensures that the depositional environments and processes, and how these may influence the ages, are well understood. Some of these methods, such as Schmidt Hammer dating, may be useful to assess and select samples for expensive methods such as cosmogenic nuclide dating. Techniques such as careful morphostratigraphy may be used to correlate between radiometrically dated and un-dated moraines, allowing ice margins to be reconstructed over a much wider spatial area.

Relevant Websites

- http://www.shed.earth/shedcalc/ (accessed on 17.02.2020). *SHED Earth.* Online calculator for Schmidt hammer exposure age dating.
- http://www.antarcticglaciers.org/glacial-geology/dating-glacial-sediments-2/ (accessed on 01.02.2020). Accessible articles on the dating of glacial environments.

Acknowledgements

Davies acknowledges Malcolm Kelsey for assistance in producing some of the figures and graphics. Davies acknowledges fruitful discussions with many colleagues over several years that aided the development of the quality assurance protocols, methods for analyzing and presenting chronological data, and all colleagues who contributed to remote, challenging fieldwork and the gathering of datasets.

List of Figures

List of Tables

References

Abbott, P.M., Bourne, A.J., Purcell, C.S., Davies, S.M., Scourse, J.D., Pearce, N.J.G., 2016. Last glacial period cryptotephra deposits in an eastern North Atlantic marine sequence: Exploring linkages to the Greenland ice-cores. Quat. Geochronol. 31, 62–76. https://doi.org/https://doi.org/10.1016/j.quageo.2015.11.001

Abbott, P.M., Griggs, A.J., Bourne, A.J., Davies, S.M., 2018. Tracing marine cryptotephras in the North Atlantic during the last glacial period: Protocols for identification, characterisation and evaluating depositional controls. Mar. Geol. 401, 81–97. https://doi.org/https://doi.org/10.1016/j.margeo.2018.04.008

Alloway, B. V, Lowe, D.J., Larsen, G., Shane, P.A.R., Westgate, J.A., 2013. QUATERNARY STRATIGRAPHY | Tephrochronology, in: Elias, S.A., Mock, C.J.B.T.-E. of Q.S. (Second E. (Eds.), Encyclopedia of Quaternary Science. Elsevier, Amsterdam, pp. 277–304. https://doi.org/https://doi.org/10.1016/B978-0-444-53643-3.00058-3

Andreassen, L.M., Paul, F., Kääb, A., Hausberg, J.E., 2008. Landsat-derived glacier inventory for Jotunheimen, Norway, and deduced glacier changes since the 1930s. Cryosph. 2, 131–145.

Araneda, A., Torrejon, F., Aguayo, M., Torres, L., Cruces, F., Cisternas, M., Urrutia, R., 2007. Historical records of San Rafael glacier advances (North Patagonian Icefield): another clue to "Little Ice Age" timing in southern Chile? Holocene 17, 987–998. https://doi.org/10.1177/0959683607082414

Barclay, D.J., Barclay, J.L., Calkin, P.E., Wiles, G.C., 2006. A revised and extended Holocene glacial history of Icy Bay, southern Alaska, USA. Arctic, Antarct. Alp. Res. 38, 153–162.

Barclay, D.J., Wiles, G.C., Calkin, P.E., 2009. Tree-ring crossdates for a First Millennium AD advance of Tebenkof Glacier, southern Alaska. Quat. Res. 71, 22–26.

Barr, I.D., Lovell, H., 2014. A review of topographic controls on moraine distribution. Geomorphology 226, 44–64. https://doi.org/https://doi.org/10.1016/j.geomorph.2014.07.030

Barr, I.D., Roberson, S., Flood, R., Dortch, J., 2017. Younger Dryas glaciers and climate in the Mourne Mountains, Northern Ireland. J. Quat. Sci. 32, 104–115. https://doi.org/10.1002/jqs.2927

Bendle, J.M., Palmer, A.P., Carr, S.J., 2015. A comparison of micro-CT and thin section analysis of Lateglacial glaciolacustrine varves from Glen Roy, Scotland. Quat. Sci. Rev. 114, 61–77. https://doi.org/http://dx.doi.org/10.1016/j.quascirev.2015.02.008

Bendle, J.M., Palmer, A.P., Thorndycraft, V.R., Matthews, I.P., 2019. Phased Patagonian Ice Sheet response to Southern Hemisphere atmospheric and oceanic warming between 18 and 17 ka. Sci. Rep. 9, 4133. https://doi.org/10.1038/s41598-019-39750-w

Bendle, J.M., Palmer, A.P., Thorndycraft, V.R., Matthews, I.P., 2017. High-resolution chronology for deglaciation of the Patagonian Ice Sheet at Lago Buenos Aires (46.5°S) revealed through varve chronology and Bayesian age modelling. Quat. Sci. Rev. 177, 314–339. https://doi.org/https://doi.org/10.1016/j.quascirev.2017.10.013

Benedict, J.B., 2009. A review of lichenometric dating and its applications to archaeology. Am. Antiq. 74, 143–172.

Benn, D.I., Owen, L.A., 2002. Himalayan glacial sedimentary environments: a framework for reconstructing and dating the former extent of glaciers in high mountains. Quat. Int. 97–98, 3–25.

Berg, S., Melles, M., Hermichen, W., McClymont, E.L., Bentley, M.J., Hodgson, D.A., Kuhn, G., 2019. Evaluation of mumiyo deposits from East Antarctica as archives for the Late Quaternary environmental and climatic history. Geochemistry, Geophys. Geosystems 20, 260–276.

Beschel, R.E., 1950. Flechten als Altersmaßstab rezenter Moränen. Zeitschrift für Gletscherkd. und Glazialgeol. 1, 152–161.

Bickerdike, H.L., Ó Cofaigh, C., Evans, D.J.A., Stokes, C.R., 2018. Glacial landsystems, retreat dynamics and controls on Loch Lomond Stadial (Younger Dryas) glaciation in Britain. Boreas 47, 202–224. https://doi.org/10.1111/bor.12259

Blockley, S.P.E., Bourne, A.J., Brauer, A., Davies, S.M., Hardiman, M., Harding, P.R., Lane, C.S., MacLeod, A., Matthews, I.P., Pyne-O'Donnell, S.D.F., 2014. Tephrochronology and the extended intimate (integration

of ice-core, marine and terrestrial records) event stratigraphy 8–128 ka b2k. Quat. Sci. Rev. 106, 88–100.

Boninsegna, J.A., Argollo, J., Aravena, J.C., Barichivich, J., Christie, D., Ferrero, M.E., Lara, A., Le Quesne, C., Luckman, B.H., Masiokas, M., Morales, M., Oliveira, J.M., Roig, F., Srur, A., Villalba, R., 2009. Dendroclimatological reconstructions in South America: A review. Palaeogeogr. Palaeoclimatol. Palaeoecol. 281, 210–228. https://doi.org/10.1016/j.palaeo.2009.07.020

Boston, C.M., Lukas, S., 2017. Evidence for restricted Loch Lomond Stadial plateau ice in Glen Turret and implications for the age of the Turret Fan. Proc. Geol. Assoc. 128, 42–53. https://doi.org/https://doi.org/10.1016/j.pgeola.2016.03.008

Boston, C.M., Lukas, S., Carr, S.J., 2015. A Younger Dryas plateau icefield in the Monadhliath, Scotland, and implications for regional palaeoclimate. Quat. Sci. Rev. 108, 139–162. https://doi.org/http://dx.doi.org/10.1016/j.quascirev.2014.11.020

Bradwell, T., 2009. Lichenometric dating: a commentary, in the light of some recent statistical studies. Geogr. Ann. Ser. A, Phys. Geogr. 91, 61–69.

Bradwell, T., Dugmore, A.J., Sugden, D.E., 2006. The little ice age glacier maximum in Iceland and the North Atlantic Oscillation: Evidence from Lambatungnajökull, southeast Iceland. Boreas 35, 61–80.

Bridgland, D.R., 2000. River terrace systems in north-west Europe: an archive of environmental change, uplift and early human occupation. Quat. Sci. Rev. 19, 1293–1303.

Bridgland, D.R., Preece, R.C., Roe, H.M., Tipping, R.M., Coope, G.R., Field, M.H., Robinson, J.E., Schreve, D.C., Crowe, K., 2001. Middle Pleistocene interglacial deposits at Barling, Essex, England: evidence for a longer chronology for the Thames terrace sequence. J. Quat. Sci. 16, 813–840.

Briner, J.P., 2011. Dating glacial landforms, in: Singh, V.P., Singh, P., Haritashya, U.K. (Eds.), Encyclopedia of Snow, Ice and Glaciers. Springer, pp. 175–186.

Bull, W.B., 2018. Accurate surface exposure dating with lichens. Quat. Res. 90, 1–9. https://doi.org/DOI: 10.1017/qua.2018.7

Bull, W.B., Brandon, M.T., 1998. Lichen dating of earthquake-generated regional rockfall events, Southern Alps, New Zealand. Geol. Soc. Am. Bull. 110, 60–84.

Caldenius, C.C., 1932. Las glaciaciones cuaternarias en la Patagonia y Tierra del Fuego. Geogr. Ann. 14, 1–164.

Chandler, B.M.P., Boston, C.M., Lukas, S., 2019. A spatially-restricted Younger Dryas plateau icefield in the Gaick, Scotland: Reconstruction and palaeoclimatic implications. Quat. Sci. Rev. 211, 107–135.

Chandler, B.M.P., Lovell, H., Boston, C.M., Lukas, S., Barr, I.D., Benediktsson, Í.Ö., Benn, D.I., Clark, C.D., Darvill, C.M., Evans, D.J.A., Ewertowski, M.W., Loibl, D., Margold, M., Otto, J.-C., Roberts, D.H., Stokes, C.R., Storrar, R.D., Stroeven, A.P., 2018. Glacial geomorphological mapping: A review of approaches and frameworks for best practice. Earth-Science Rev. 185, 806–846. https://doi.org/https://doi.org/10.1016/j.earscirev.2018.07.015

Clapperton, C.M., 1995. Fluctuations of local glaciers at the termination of the Pleistocene: 18-8 ka BP. Quat.

Int. 28, 41–50.

Cook, A.J., Fox, A.J., Vaughan, D.G., Ferrigno, J.G., 2005. Retreating glacier fronts on the Antarctic Peninsula over the past half-century. Science (80-.). 308, 541–544. https://doi.org/DOI: 10.1126/science.1104235

Cook, A.J., Vaughan, D.G., Luckman, A.J., Murray, T., 2014. A new Antarctic Peninsula glacier basin inventory and observed area changes since the 1940s. Antarct. Sci. 26, 614–624. https://doi.org/doi:10.1017/S0954102014000200

Cook, E., Portnyagin, M., Ponomareva, V., Bazanova, L., Svensson, A., Garbe-Schönberg, D., 2018. First identification of cryptotephra from the Kamchatka Peninsula in a Greenland ice core: Implications of a widespread marker deposit that links Greenland to the Pacific northwest. Quat. Sci. Rev. 181, 200–206. https://doi.org/https://doi.org/10.1016/j.quascirev.2017.11.036

Coulthard, B., Smith, D.J., Lacourse, T., 2013. Dendroglaciological investigations of mid-to late-Holocene glacial activity in the Mt. Waddington area, British Columbia Coast Mountains, Canada. The Holocene 23, 93–103.

Coulthard, B.L., Smith, D.J., 2013. Dendroglaciology , in: Elias, S.A. (Ed.), Encyclopedia of Quaternary Science (Second Edition). Elsevier, Amsterdam, pp. 104–111. https://doi.org/https://doi.org/10.1016/B978-0-444-53643-3.00357-5

Dalton, A.S., Margold, M., Stokes, C.R., Tarasov, L., Dyke, A.S., Adams, R.S., Allard, S., Arends, H.E., Atkinson, N., Attig, J.W., Barnett, P.J., Barnett, R.L., Batterson, M., Bernatchez, P., Borns, H.W., Breckenridge, A., Briner, J.P., Brouard, E., Campbell, J.E., Carlson, A.E., Clague, J.J., Curry, B.B., Daigneault, R.-A., Dubé-Loubert, H., Easterbrook, D.J., Franzi, D.A., Friedrich, H.G., Funder, S., Gauthier, M.S., Gowan, A.S., Harris, K.L., Hétu, B., Hooyer, T.S., Jennings, C.E., Johnson, M.D., Kehew, A.E., Kelley, S.E., Kerr, D., King, E.L., Kjeldsen, K.K., Knaeble, A.R., Lajeunesse, P., Lakeman, T.R., Lamothe, M., Larson, P., Lavoie, M., Loope, H.M., Lowell, T. V, Lusardi, B.A., Manz, L., McMartin, I., Nixon, F.C., Occhietti, S., Parkhill, M.A., Piper, D.J.W., Pronk, A.G., Richard, P.J.H., Ridge, J.C., Ross, M., Roy, M., Seaman, A., Shaw, J., Stea, R.R., Teller, J.T., Thompson, W.B., Thorleifson, L.H., Utting, D.J., Veillette, J.J., Ward, B.C., Weddle, T.K., Wright, H.E., 2020. An updated radiocarbon-based ice margin chronology for the last deglaciation of the North American Ice Sheet Complex. Quat. Sci. Rev. 234, 106223. https://doi.org/https://doi.org/10.1016/j.quascirev.2020.106223

Davies, B.J., Bridgland, D.R., Roberts, D.H., Cofaigh, C.O., Pawley, S.M., Candy, I., Demarchi, B., Penkman, K.E.H., Austin, W.E.N., 2009. The age and stratigraphic context of the Easington Raised Beach, County Durham, UK. Proc. Geol. Assoc. 120. https://doi.org/10.1016/j.pgeola.2009.04.001

Davies, B.J., Darvill, C.M., Lovell, H., Bendle, J.M., Dowdeswell, J.A., Fabel, D., Garcia, J.L., Geiger, A., Glasser, N.F., Gheorghiu, D.M., Harrison, S., Hein, A.S., Martin, J.R.V., Mendelová, M., Palmer, A., Pelto, M.S., Rodes, A., Sagredo, E.A., Smedley, R.K., Smellie, J.L., Thorndycraft, V.R., 2020. The evolution of the Patagonian Ice Sheet from 35 ka to the present day (PATICE). Earth-Science Rev. 204, 103152.

Davies, B.J., Glasser, N.F., 2012a. Accelerating recession in Patagonian glaciers from the “Little Ice Age” (c. AD 1870) to 2011. J. Glaciol. 58, 1063–1084. https://doi.org/10.3189/2012JoG12J026

Davies, B.J., Glasser, N.F., 2012b. Accelerating shrinkage of Patagonian glaciers from the Little Ice Age (∼AD 1870) to 2011. J. Glaciol. 58. https://doi.org/10.3189/2012JoG12J026

Davies, B.J., Thorndycraft, V.R., Fabel, D., Martin, J.R.V., 2018. Asynchronous glacier dynamics during the Antarctic Cold Reversal in central Patagonia. Quat. Sci. Rev. 200. https://doi.org/10.1016/j.quascirev.2018.09.025

Davies, S.M., 2015. Cryptotephras: the revolution in correlation and precision dating. J. Quat. Sci. 30, 114–130.

Davies, S.M., Abbott, P.M., Pearce, N.J.G., Wastegård, S., Blockley, S.P.E., 2012. Integrating the INTIMATE records using tephrochronology: rising to the challenge. Quat. Sci. Rev. 36, 11–27.

Demarchi, B., Collins, M.J., Tomiak, P.J., Davies, B.J., Penkman, K.E.H., 2012. Intra-crystalline protein diagenesis (IcPD) in Patella vulgata. Part II: Breakdown and temperature sensitivity. Quat. Geochronol. 1014–1871. https://doi.org/http://dx.doi.org/10.1016/j.quageo.2012.08.001

Devine, R.M., Palmer, A.P., 2017. A new varve thickness record from Allt Bhraic Achaidh Fan, middle Glen Roy, Lochaber: implications for understanding the Loch Lomond Stadial glaciolacustrine varve sedimentation trends. Proc. Geol. Assoc. 128, 136–145. https://doi.org/https://doi.org/10.1016/j.pgeola.2016.07.008

Di Roberto, A., Colizza, E., Del Carlo, P., Petrelli, M., Finocchiaro, F., Kuhn, G., 2019. First marine cryptotephra in Antarctica found in sediments of the western Ross Sea correlates with englacial tephras and climate records. Sci. Rep. 9, 10628. https://doi.org/10.1038/s41598-019-47188-3

Dortch, J.M., Hughes, P.D., Tomkins, M.D., 2016. Schmidt hammer exposure dating (SHED): Calibration boulder of. Quat. Geochronol. 35, 7e68.

Douglass, A.E., 1914. A method of estimating rainfall by the growth of trees. Bull. Am. Geogr. Soc. 46, 321–335.

Douglass, D.C., Singer, B.S., Kaplan, M.R., Mickelson, D.M., Caffee, M.W., 2006. Cosmogenic nuclide surface exposure dating of boulders on last-glacial and late-glacial moraines, Lago Buenos Aires, Argentina: interpretive strategies and paleoclimate implications. Quat. Geochronol. 1, 43–58.

Duk-Rodkin, A., Barendregt, R.W., Tarnocai, C., Phillips, F.M., 1996. Late Tertiary to late Quaternary record in the Mackenzie Mountains, Northwest Territories, Canada: stratigraphy, paleosols, paleomagnetism, and chlorine-36. Can. J. Earth Sci. 33, 875–895.

Dyke, A.S., Moore, A., Robertson, L., 2003. Deglaciation of North America. Geological Survey of Canada Ottawa, ON.

Ely, J.C., Clark, C.D., Hindmarsh, R.C.A., Hughes, A.L.C., Greenwood, S.L., Bradley, S.L., Gasson, E., Gregoire, L., Gandy, N., Stokes, C.R., 2019. Recent progress on combining geomorphological and geochronological data with ice sheet modelling, demonstrated using the last British–Irish Ice Sheet. J. Quat. Sci.

Evans, D.J.A., 2007. GLACIAL LANDFORMS | Glacial Land Systems, in: Scott, E. (Ed.), Encyclopedia of Quaternary Science. Elsevier, Oxford, pp. 808–818. https://doi.org/http://dx.doi.org/10.1016/B0-44-452747-8/00096-X

Evans, D.J.A., 2004. Glacial Landsystems. Hodder, London.

Evans, D.J.A., Archer, S., Wilson, D.J.H., 1999. A comparison of the lichenometric and Schmidt hammer dating techniques based on data from the proglacial areas of some Icelandic glaciers. Quat. Sci. Rev. 18, 13–41. https://doi.org/http://dx.doi.org/10.1016/S0277-3791(98)00098-5

Evans, D.J.A., Twigg, D.R., 2002. The active temperate glacial landsystem: a model based on Breiethamerkurjokull and Fjallsjokull, Iceland. Quat. Sci. Rev. 21, 2143–2177.

Ferrigno, J.G., Cook, A.J., Foley, K.M., Williams, R.S., Swithinbank, C., Fox, A.J., Thomson, J.W., Sievers, J., 2006. Coastal-Change and Glaciological Map of the Trinity Peninsula Area and South Shetland Islands, Antarctica: 1843-2001, Geological Investigations Series, I-2600-A. USGS, Denver.

Ffoulkes, C., Harrison, S., 2014. Evaluating the Schmidt hammer as a method for distinguishing the relative age of late Holocene moraines: Svellnosbreen, Jotunheimen, Norway. Geogr. Ann. Ser. A, Phys. Geogr. 96, 393–402.

Fontijn, K., Rawson, H., Van Daele, M., Moernaut, J., Abarzúa, A.M., Heirman, K., Bertrand, S., Pyle, D.M., Mather, T.A., De Batist, M., Naranjo, J.A., Moreno, H., 2016. Synchronisation of sedimentary records using tephra: A postglacial tephrochronological model for the Chilean Lake District. Quat. Sci. Rev. 137, 234–254. https://doi.org/10.1016/j.quascirev.2016.02.015

Freudiger, D., Mennekes, D., Seibert, J., Weiler, M., 2018. Historical glacier outlines from digitized topographic maps of the Swiss Alps. Earth Syst. Sci. Data 10, 805–814.

Frey, H., Huggel, C., Paul, F., Haeberli, W., 2010. Automated detection of glacier lakes based on remote sensing in view of assessing associated hazard potentials. Grazer Schriften der Geogr. und Raumforsch. Band 44, 23–30.

Gardent, M., Rabatel, A., Dedieu, J.-P., Deline, P., 2014. Multitemporal glacier inventory of the French Alps from the late 1960s to the late 2000s. Glob. Planet. Change 120, 24–37.

Garibotti, I.A., Villalba, R., 2017. Colonization of mid- and late-Holocene moraines by lichens and trees in the Magellanic sub-Antarctic province. Polar Biol. 1–15. https://doi.org/10.1007/s00300-017-2096-1 LB - Garibotti2017

Garibotti, I.A., Villalba, R., 2009. Lichenometric dating using Rhizocarpon subgenus Rhizocarpon in the Patagonian Andes, Argentina. Quat. Res. 71, 271–283.

Gibbard, P.L., Clark, C.D., 2011. Pleistocene glaciation limits in Great Britain, in: Developments in Quaternary Sciences. Elsevier, pp. 75–93.

Glasser, N.F., Harrison, S., Jansson, K.N., Anderson, K., Cowley, A., 2011. Global sea-level contribution from the Patagonian Icefields since the Little Ice Age maximum. Nat. Geosci. 4, 303–307. https://doi.org/10.1038/ngeo1122

Glasser, N.F., Holt, T.O., Evans, Z.D., Davies, B.J., Pelto, M., Harrison, S., 2016. Recent spatial and temporal variations in debris cover on Patagonian glaciers. Geomorphology 273. https://doi.org/10.1016/j.geomorph.2016.07.036

Goudie, A.S., 2006. The Schmidt Hammer in geomorphological research. Prog. Phys. Geogr. 30, 703–718. https://doi.org/10.1177/0309133306071954

Granshaw, F.D., Fountain, A.G., 2006. Glacier change (1958-1998) in the North Cascades National Park Complex, Washington, USA. J. Glaciol. 52, 251–256.

Harrison, S., Winchester, V., Glasser, N., 2007. The timing and nature of recession of outlet glaciers of Hielo Patagonico Norte, Chile, from their Neoglacial IV (Little Ice Age) maximum positions. Glob. Planet. Change 59, 67–78. https://doi.org/10.1016/j.gloplacha.2006.11.020

Hein, A.S., Cogez, A., Darvill, C.M., Mendelova, M., Kaplan, M.R., Herman, F., Dunai, T.J., Norton, K., Xu, S., Christl, M., 2017. Regional mid-Pleistocene glaciation in central Patagonia. Quat. Sci. Rev. 164, 77–94.

Hughes, A.L.C., Gyllencreutz, R., Lohne, Ø.S., Mangerud, J., Svendsen, J.I., 2016. The last Eurasian ice sheets–a chronological database and time-slice reconstruction, DATED-1. Boreas 45, 1–45.

Izagirre, E., Darvill, C.M., Rada, C., Aravena, J.C., 2018. Glacial geomorphology of the Marinelli and Pigafetta glaciers, Cordillera Darwin Icefield, southernmost Chile. J. Maps 14, 269–281.

Jackson, S.I., Laxton, S.C., Smith, D.J., 2008. Dendroglaciological evidence for Holocene glacial advances in the Todd Icefield area, northern British Columbia Coast Mountains. Can. J. Earth Sci. 45, 83–98.

Jull, A.J.T., 2018. Chapter 19 - Geochronology Applied to Glacial Environments, in: Menzies, J., van der Meer, J.J.M. (Eds.), Past Glacial Environments (Second Edition). Elsevier, pp. 665–687. https://doi.org/https://doi.org/10.1016/B978-0-08-100524-8.00020-8

Kaplan, M.R., Ackert, R.P., Singer, B.S., Douglass, D.C., Kurz, M.D., 2004. Cosmogenic nuclide chronology of millennial-scale glacial advances during O-isotope stage 2 in Patagonia. GSA Bull. 116, 308–321. https://doi.org/10.1130/b25178.1

Kaufman, D.S., Cooper, K., Behl, R., Billups, K., Bright, J., Gardner, K., Hearty, P., Jakobsson, M., Mendes, I., O'Leary, M., 2013. Amino acid racemization in mono-specific foraminifera from Quaternary deep-sea sediments. Quat. Geochronol. 16, 50–61.

Kienholz, C., Herreid, S., Rich, J.L., Arendt, A.A., Hock, R., Burgess, E.W., 2015. Derivation and analysis of a complete modern-date glacier inventory for Alaska and northwest Canada. J. Glaciol. 61, 403–420.

Kilian, R., Hohner, M., Biester, H., Wallrabe-Adams, H.J., Stern, C.R., 2003. Holocene peat and lake sediment tephra record from the southernmost Chilean Andes (53-55 S). Rev. Geol. Chile 30, 23–37.

Kilian, R., Lamy, F., Arz, H., 2013. Late Quaternary variations of the southern westerly wind belt and its influences on aquatic ecosystems and glacier extend within the southernmost Andes [Spätquartäre Variationen der südhemisphärischen Westwindzone und deren Einfluss auf aquatische Ökosyst. Zeitschrift der Dtsch. Gesellschaft für Geowissenschaften 164, 279–294.

Kilian, R., Schneider, C., Koch, J., Fesq-Martin, M., Biester, H., Casassa, G., Arévalo, M., Wendt, G., Baeza, O., Behrmann, J., 2007. Palaeoecological constraints on late Glacial and Holocene ice retreat in the Southern Andes (53°S). Glob. Planet. Change 59, 49–66. https://doi.org/http://dx.doi.org/10.1016/j.gloplacha.2006.11.034

Kirkbride, M.P., Dugmore, A.J., 2008. Two millennia of glacier advances from southern Iceland dated by tephrochronology. Quat. Res. 70, 398–411.

Kirkbride, M.P., Dugmore, A.J., 2003. Glaciological response to distal tephra fallout from the 1947 eruption

of Hekla, south Iceland. J. Glaciol. 49, 420–428.

Kirkbride, M.P., Winkler, S., 2012. Correlation of Late Quaternary moraines: impact of climate variability, glacier response, and chronological resolution. Quat. Sci. Rev. 46, 1–29. https://doi.org/http://dx.doi.org/10.1016/j.quascirev.2012.04.002

Koch, J., 2009. Improving age estimates for late Holocene glacial landforms using dendrochronology–Some examples from Garibaldi Provincial Park, British Columbia. Quat. Geochronol. 4, 130–139.

Koch, J., Kilian, R., 2005. "Little Ice Age" glacier fluctuations, Gran Campo Nevado, southernmost Chile. Holocene 15, 20–28. https://doi.org/10.1191/0959683605hl780rp

Koehler, L., Smith, D.J., 2011. Late Holocene glacial activity in Manatee Valley, southern Coast Mountains, British Columbia, Canada. Can. J. Earth Sci. 48, 603–618.

Lane, C.S., Lowe, D.J., Blockley, S.P.E., Suzuki, T., Smith, V.C., 2017. Advancing tephrochronology as a global dating tool: applications in volcanology, archaeology, and palaeoclimatic research.

Larsen, D.J., Miller, G.H., Geirsdóttir, Á., Ólafsdóttir, S., 2012. Non-linear Holocene climate evolution in the North Atlantic: a high-resolution, multi-proxy record of glacier activity and environmental change from Hvítárvatn, central Iceland. Quat. Sci. Rev. 39, 14–25.

Le Bris, R., Paul, F., 2013. An automatic method to create flow lines for determination of glacier length: A pilot study with Alaskan glaciers. Comput. Geosci. 52, 234–245. https://doi.org/http://dx.doi.org/10.1016/j.cageo.2012.10.014

Lee, J.R., Booth, S.J., Hamblin, R.J.O., Jarrow, A.M., Kessler, H.K.E., Moorlock, B.S.P., Morigi, A.M., Palmer, A., Pawley, S.M., Riding, J.B., Rose, J., 2004. A new stratigraphy for the glacial deposits around Lowestoft, Great Yarmouth and Cromer, East Anglia, UK. Bull. Geol. Soc. Norfolk 53, 3–60.

Lee, J.R., Rose, J., Hamblin, R.J.O., Moorlock, B.S.P., Riding, J.B., Phillips, E., Barendregt, R.W., Candy, I., 2011. The Glacial History of the British Isles during the Early and Middle Pleistocene: Implications for the long-term development of the British Ice Sheet, in: Developments in Quaternary Sciences. Elsevier, pp. 59–74.

Lowe, D.J., 2011. Tephrochronology and its application: a review. Quat. Geochronol. 6, 107–153.

Lowe, J., Matthews, I., Mayfield, R., Lincoln, P., Palmer, A., Staff, R., Timms, R., 2019. On the timing of retreat of the Loch Lomond ('Younger Dryas') Readvance icefield in the SW Scottish Highlands and its wider significance. Quat. Sci. Rev. 219, 171–186.

Lowe, J.J., Ramsey, C.B., Housley, R.A., Lane, C.S., Tomlinson, E.L., Associates, R., Team, R., 2015. The RESET project: constructing a European tephra lattice for refined synchronisation of environmental and archaeological events during the last c. 100 ka. Quat. Sci. Rev. 118, 1–17.

Lowe, J.J., Rasmussen, S.O., Björck, S., Hoek, W.Z., Steffensen, J.P., Walker, M.J.C., Yu, Z.C., 2008. Synchronisation of palaeoenvironmental events in the North Atlantic region during the Last Termination: a revised protocol recommended by the INTIMATE group. Quat. Sci. Rev. 27, 6–17. https://doi.org/https://doi.org/10.1016/j.quascirev.2007.09.016

Lowe, J.J., Walker, M.J.C., 2014. Reconstructing Quaternary Environments. Addison Wesley Longman,

London.

Lukas, S., 2006. Morphostratigraphic principles in glacier reconstruction - a perspective from the British Younger Dryas. Prog. Phys. Geogr. 30, 719–736. https://doi.org/10.1177/0309133306071955

Lukas, S., Spencer, J.Q.G., Robinson, R.A.J., Benn, D.I., 2007. Problems associated with luminescence dating of Late Quaternary glacial sediments in the NW Scottish Highlands. Quat. Geochronol. 2, 243–248. https://doi.org/https://doi.org/10.1016/j.quageo.2006.04.007

Lüthgens, C., Böse, M., 2012. From morphostratigraphy to geochronology–on the dating of ice marginal positions. Quat. Sci. Rev. 44, 26–36.

MacLeod, A., Matthews, I.P., Lowe, J.J., Palmer, A.P., Albert, P.G., 2015. A second tephra isochron for the Younger Dryas period in northern Europe: The Abernethy Tephra. Quat. Geochronol. 28, 1–11. https://doi.org/http://dx.doi.org/10.1016/j.quageo.2015.03.010

Magee, J.W., Miller, G.H., Spooner, N.A., Questiaux, D.G., McCulloch, M.T., Clark, P.A., 2009. Evaluating Quaternary dating methods: Radiocarbon, U-series, luminescence, and amino acid racemization dates of a late Pleistocene emu egg. Quat. Geochronol. 4, 84–92. https://doi.org/https://doi.org/10.1016/j.quageo.2008.10.001

Mahaney, W.C., Barendregt, R.W., Hamilton, T.S., Hancock, R.G. V, Tessler, D., Costa, P.J.M., 2013. Stratigraphy of the Gorges moraine system, Mount Kenya: palaeosol and palaeoclimate record. J. Geol. Soc. London. 170, 497–511.

Malz, P., Meier, W., Casassa, G., Jaña, R., Skvarca, P., Braun, M., 2018. Elevation and mass changes of the Southern Patagonia Icefield derived from TanDEM-X and SRTM data. Remote Sens. 10, 188.

Marr, P., Winkler, S., Löffler, J., 2018. Investigations on blockfields and related landforms at Blåhø (Southern Norway) using Schmidt-hammer exposure-age dating: palaeoclimatic and morphodynamic implications. Geogr. Ann. Ser. A, Phys. Geogr. 100, 285–306.

Masiokas, M.H., Rivera, A., Espizua, L.E., Villalba, R., Delgado, S., Aravena, J.C., 2009. Glacier fluctuations in extratropical South America during the past 1000 years. Palaeogeogr. Palaeoclimatol. Palaeoecol. 281, 242–268.

Matthews, I.P., Trincardi, F., Lowe, J.J., Bourne, A.J., MacLeod, A., Abbott, P.M., Andersen, N., Asioli, A., Blockley, S.P.E.E., Lane, C.S., Oh, Y.A., Satow, C.S., Staff, R.A., Wulf, S., 2015. Developing a robust tephrochronological framework for Late Quaternary marine records in the Southern Adriatic Sea: new data from core station SA03-11. Quat. Sci. Rev. 118, 84–104. https://doi.org/https://doi.org/10.1016/j.quascirev.2014.10.009

Matthews, J.A., Owen, G., 2010. Schmidt hammer exposure-age dating: developing linear age-calibration curves using Holocene bedrock surfaces from the Jotunheimen–Jostedalsbreen regions of southern Norway. Boreas 39, 105–115.

McCarthy, D.P., 2013. LICHENOMETRY, in: Elias, S.A., Mock, C.J.B.T. (Eds.), Encyclopedia of Quaternary Science (Second Edition). Elsevier, Amsterdam, pp. 565–572. https://doi.org/https://doi.org/10.1016/B978-0-444-53643-3.00055-8

Meier, W.J.-H., Grießinger, J., Hochreuther, P., Braun, M.H., 2018. An updated multi-temporal glacier

inventory for the Patagonian Andes with changes between the Little Ice Age and 2016. Front. Earth Sci. 6, 1–21.

Mendelová, M., Hein, A.S., Rodés, Á., Xu, S., 2020. Extensive mountain glaciation in central Patagonia during Marine Isotope Stage 5. Quat. Sci. Rev. 227, 105996.

Mercer, J.H., 1972. Chilean glacial chronology 20,000 to 11,000 carbon-14 years ago: some global comparisons. Science (80-.). 176, 1118–1120.

Monteath, A.J., Hughes, P.D.M., Wastegård, S., 2019. Evidence for distal transport of reworked Andean tephra: Extending the cryptotephra framework from the Austral volcanic zone. Quat. Geochronol. 51, 64–71. https://doi.org/https://doi.org/10.1016/j.quageo.2019.01.003

Mörner, N.-A., Sylwan, C., 1989. Magnetostratigraphy of the Patagonian moraine sequence at Lago Buenos Aires. J. South Am. Earth Sci. 2, 385–389. https://doi.org/https://doi.org/10.1016/0895-9811(89)90016-3

Nussbaumer, S.U., Zumbühl, H.J., 2012. The Little Ice Age history of the Glacier des Bossons (Mont Blanc massif, France): a new high-resolution glacier length curve based on historical documents. Clim. Change 111, 301–334.

Nuth, C., Kohler, J., König, M., Deschwanden, A. von, Hagen, J.O.M., Kääb, A., Moholdt, G., Pettersson, R., 2013. Decadal changes from a multi-temporal glacier inventory of Svalbard. Cryosph. 7, 1603–1621.

O'Neel, S., McNeil, C., Sass, L.C., Florentine, C., Baker, E.H., Peitzsch, E., McGrath, D., Fountain, A.G., Fagre, D., 2019. Reanalysis of the US Geological Survey Benchmark Glaciers: long-term insight into climate forcing of glacier mass balance. J. Glaciol. 65, 850–866. https://doi.org/DOI: 10.1017/jog.2019.66

Ojala, A.E.K., Francus, P., Zolitschka, B., Besonen, M., Lamoureux, S.F., 2012. Characteristics of sedimentary varve chronologies–a review. Quat. Sci. Rev. 43, 45–60.

Osborn, G., McCarthy, D., LaBrie, A., Burke, R., 2015. Lichenometric dating: Science or pseudo-science? Quat. Res. 83, 1–12. https://doi.org/http://dx.doi.org/10.1016/j.yqres.2014.09.006

Palmer, A.P., Rose, J., Lowe, J.J., MacLeod, A., 2010. Annually resolved events of Younger Dryas glaciation in Lochaber (Glen Roy and Glen Spean), western Scottish Highlands. J. Quat. Sci. 25, 581–596. https://doi.org/10.1002/jqs.1370

Palmer, A.P., Rose, J., Rasmussen, S.O., 2012. Evidence for phase-locked changes in climate between Scotland and Greenland during GS-1 (Younger Dryas) using micromorphology of glaciolacustrine varves from Glen Roy. Quat. Sci. Rev. 36, 114–123. https://doi.org/http://dx.doi.org/10.1016/j.quascirev.2011.12.003

Paul, F., Barry, R.G., Cogley, J.G., Frey, H., Haeberli, W., Ohmura, A., Ommanney, C.S.L., Raup, B., Rivera, A., Zemp, M., 2010. Guidelines for the compliation of glacier inventory data from digital sources. GLIMS, Global Land Ice Measurement from Space, NSIDC, University of Colorado, Boulder.

Paul, F., Bolch, T., Kääb, A., Nagler, T., Nuth, C., Scharrer, K., Shepherd, A., Strozzi, T., Ticconi, F., Bhambri, R., Berthier, E., Bevan, S., Gourmelen, N., Heid, T., Jeong, S., Kunz, M., Lauknes, T.R., Luckman, A., Merryman, J., Moholdt, G., Muir, A., Neelmeijer, J., Rankl, M., VanLooy, J., Van Niel, T., 2013. The glaciers climate change initiative: Methods for creating glacier area, elevation change and velocity

products. Remote Sens. Environ. in press. https://doi.org/http://dx.doi.org/10.1016/j.rse.2013.07.043

Penkman, K., 2010. Amino acid geochronology: its impact on our understanding of the Quaternary stratigraphy of the British Isles. J. Quat. Sci. Publ. Quat. Res. Assoc. 25, 501–514.

Penkman, K.E.H., Kaufman, D.S., Maddy, D., Collins, M.J., 2008. Closed-system behaviour of the intra-crystalline fraction of amino acids in mollusc shells. Quat. Geochronol. 3, 2–25.

Penkman, K.E.H., Preece, R.C., Bridgland, D.R., Keen, D.H., Meijer, T., Parfitt, S.A., White, T.S., Collins, M.J., 2013. An aminostratigraphy for the British Quaternary based on Bithynia opercula. Quat. Sci. Rev. 61, 111–134. https://doi.org/http://dx.doi.org/10.1016/j.quascirev.2012.10.046

Penkman, K.E.H., Preece, R.C., Bridgland, D.R., Keen, D.H., Meijer, T., Parfitt, S.A., White, T.S., Collins, M.J., 2011. A chronological framework for the British Quaternary based on Bithynia opercula. Nature 476, 446–449. https://doi.org/http://www.nature.com/nature/journal/v476/n7361/abs/nature10305.html#supplementary-information

Penkman, K.E.H., Preece, R.C., Keen, D.H., Collins, M.J., 2010. Amino acid geochronology of the type Cromerian of West Runton, Norfolk, UK. Quat. Int. 228, 25–37.

Pfeffer, W.T., Arendt, A.A., Bliss, A., Bolch, T., Cogley, J.G., Gardner, A.S., Hagen, J.-O., Hock, R., Kaser, G., Kienholz, C., Miles, E.S., Moholdt, G., Mölg, N., Paul, F., Radić, V., Rastner, P., Raup, B.H., Rich, J., Sharp, M.J., Andreassen, L.M., Bajracharya, S., Barrand, N.E., Beedle, M.J., Berthier, E., Bhambri, R., Brown, I., Burgess, D.O., Burgess, E.W., Cawkwell, F., Chinn, T., Copland, L., Cullen, N.J., Davies, B., De Angelis, H., Fountain, A.G., Frey, H., Giffen, B.A., Glasser, N.F., Gurney, S.D., Hagg, W., Hall, D.K., Haritashya, U.K., Hartmann, G., Herreid, S., Howat, I., Jiskoot, H., Khromova, T.E., Klein, A., Kohler, J., König, M., Kriegel, D., Kutuzov, S., Lavrentiev, I., Le Bris, R., Li, X., Manley, W.F., Mayer, C., Menounos, B., Mercer, A., Mool, P., Negrete, A., Nosenko, G., Nuth, C., Osmonov, A., Pettersson, R., Racoviteanu, A., Ranzi, R., Sarikaya, M.A., Schneider, C., Sigurdsson, O., Sirguey, P., Stokes, C.R., Wheate, R., Wolken, G.J., Wu, L.Z., Wyatt, F.R., 2014. The Randolph Glacier Inventory: A globally complete inventory of glaciers. J. Glaciol. 60. https://doi.org/10.3189/2014JoG13J176

Preece, R.C., Parfitt, S.A., Coope, G.R., Penkman, K.E.H., Ponel, P., Whittaker, J.E., 2009. Biostratigraphic and aminostratigraphic constraints on the age of the Middle Pleistocene glacial succession in north Norfolk, UK. J. Quat. Sci. 24, 557–580.

Pritchard, H.D., Vaughan, D.G., 2007. Widespread acceleration of tidewater glaciers on the Antarctic Peninsula. J. Geophys. Res. Surf. 112, F03S29, 1-10. https://doi.org/DOI: 10.1029/2006jf000597

Rabassa, J., Coronato, A., Martinez, O., 2011. Late Cenozoic glaciations in Patagonia and Tierra del Fuego: an updated review. Biol. J. Linn. Soc. 103, 316–335.

Rabatel, A., Francou, B., Soruco, A., Gomez, J., Cáceres, B., Ceballos, J.L., Basantes, R., Vuille, M., Sicart, J.-E., Huggel, C., 2013. Current state of glaciers in the tropical Andes: a multi-century perspective on glacier evolution and climate change. Cryosph. 7, 81.

Racoviteanu, A., Williams, M.W., 2012. Decision tree and texture analysis for mapping debris-covered glaciers in the Kangchenjunga area, Eastern Himalaya. Remote Sens. 4, 3078–3109.

Racoviteanu, A.E., Williams, M.W., Barry, R.G., 2008. Optical remote sensing of glacier characteristics: a review with focus on the Himalaya. Sensors 8, 3355–3383.

Ramsey, C.B., Housley, R.A., Lane, C.S., Smith, V.C., Pollard, A.M., 2015. The RESET tephra database and associated analytical tools. Quat. Sci. Rev. 118, 33–47.

Randolph Glacier Inventory Consortium, 2017. Randolph glacier inventory–a dataset of global glacier outlines: Version 6.0: technical report, global land ice measurements from space, Colorado, USA. Digit. Media.

Rasmussen, S.O., Bigler, M., Blockley, S.P., Blunier, T., Buchardt, S.L., Clausen, H.B., Cvijanovic, I., Dahl-Jensen, D., Johnsen, S.J., Fischer, H., Gkinis, V., Guillevic, M., Hoek, W.Z., Lowe, J.J., Pedro, J.B., Popp, T., Seierstad, I.K., Steffensen, J.P., Svensson, A.M., Vallelonga, P., Vinther, B.M., Walker, M.J.C., Wheatley, J.J., Winstrup, M., 2014. A stratigraphic framework for abrupt climatic changes during the Last Glacial period based on three synchronized Greenland ice-core records: refining and extending the INTIMATE event stratigraphy. Quat. Sci. Rev. 106, 14–28. https://doi.org/http://dx.doi.org/10.1016/j.quascirev.2014.09.007

Raup, B., Kääb, A., Kargel, J.S., Bishop, M.P., Hamilton, G., Lee, E., Paul, F., Rau, F., Soltesz, D., Khalsa, S.J.S., Beedle, M., Helm, C., 2007. Remote sensing and GIS technology in the Global Land Ice Measurements from Space (GLIMS) Project. Comput. Geosci. 33, 104–125.

Ridge, J.C., Balco, G., Bayless, R.L., Beck, C.C., Carter, L.B., Dean, J.L., Voytek, E.B., Wei, J.H., 2012. The new North American Varve Chronology: A precise record of southeastern Laurentide Ice Sheet deglaciation and climate, 18.2-12.5 kyr BP, and correlations with Greenland ice core records. Am. J. Sci. 312, 685–722.

Roberts, S.J., Hodgson, D.A., Shelley, S., Royles, J., Griffiths, H.J., Deen, T.J., Thorne, M.A.S., 2010. Establishing lichenonmetric ages for nineteenth- and twentieth-century glacier fluctuations on South Georgia (South Atlantic). Geogr. Ann. Ser. A, Phys. Geogr. 92, 125–139. https://doi.org/10.1111/j.1468-0459.2010.00382.x

Roe, H.M., Coope, G.R., Devoy, R.J.N., Harrison, C.J.O., Penkman, K.E.H., Preece, R.C., Schreve, D.C., 2009. Differentiation of MIS 9 and MIS 11 in the continental record: vegetational, faunal, aminostratigraphic and sea-level evidence from coastal sites in Essex, UK. Quat. Sci. Rev. 28, 2342–2373.

Rose, J., 2010. The Quaternary of the British Isles: factors forcing environmental change. J. Quat. Sci. 25, 399–418. https://doi.org/doi:10.1002/jqs.1389

Rosenwinkel, S., Korup, O., Landgraf, A., Dzhumabaeva, A., 2015. Limits to lichenometry. Quat. Sci. Rev. 129, 229–238. https://doi.org/https://doi.org/10.1016/j.quascirev.2015.10.031

Sagredo, E.A., Moreno, P.I., Villa-Martínez, R., Kaplan, M.R., Kubik, P.W., Stern, C.R., 2011. Fluctuations of the Última Esperanza ice lobe (52°S), Chilean Patagonia, during the last glacial maximum and termination 1. Geomorphology 125, 92–108. https://doi.org/http://dx.doi.org/10.1016/j.geomorph.2010.09.007

Schaefer, J.M., Denton, G.H., Kaplan, M., Putnam, A., Finkel, R.C., Barrell, D.J.A., Andersen, B.G., Schwartz, R., Mackintosh, A., Chinn, T., SchlÃ¼chter, C., 2009. High-Frequency Holocene Glacier Fluctuations in New Zealand Differ from the Northern Signature. Science (80-.). 324, 622–625.

https://doi.org/10.1126/science.1169312

Scherler, D., Wulf, H., Gorelick, N., 2018. Global Assessment of Supraglacial Debris-Cover Extents. Geophys. Res. Lett. 45, 11,711-798,805. https://doi.org/10.1029/2018GL080158

Schreve, D.C., 2013. VERTEBRATE OVERVIEW, in: Elias, S.A., Mock, C.J.B.T.-E. of Q.S. (Second E. (Eds.), . Elsevier, Amsterdam, pp. 590–597. https://doi.org/https://doi.org/10.1016/B978-0-444-53643-3.00243-0

Schreve, D.C., 2009. A new record of Pleistocene hippopotamus from River Severn terrace deposits, Gloucester, UK--palaeoenvironmental setting and stratigraphical significance. Proc. Geol. Assoc. 120, 58–64.

Schreve, D.C., 2001. Differentiation of the British late Middle Pleistocene interglacials: the evidence from mammalian biostratigraphy. Quat. Sci. Rev. 20, 1693–1705.

Shakesby, R.A., Matthews, J.A., Owen, G., 2006. The Schmidt hammer as a relative-age dating tool and its potential for calibrated-age dating in Holocene glaciated environments. Quat. Sci. Rev. 25, 2846–2867.

Shroder Jr, J.F., 1980. Dendrogeomorphology: review and new techniques of tree-ring dating. Prog. Phys. Geogr. 4, 161–188.

Small, D., Clark, C.D., Chiverrell, R.C., Smedley, R.K., Bateman, M.D., Duller, G.A.T., Ely, J.C., Fabel, D., Medialdea, A., Moreton, S.G., 2017. Devising quality assurance procedures for assessment of legacy geochronological data relating to deglaciation of the last British-Irish Ice Sheet. Earth-Science Rev. 164, 232–250. https://doi.org/https://doi.org/10.1016/j.earscirev.2016.11.007

Smith, D., Laroque, C., 1996. Dendroglaciological dating of a Little Ice Age glacial advance at Moving Glacier, Vancouver Island, British Columbia. Géographie Phys. Quat. 50, 47–55.

Stern, C.R., 2008. Holocene tephrochronology record of large explosive eruptions in the southernmost Patagonian Andes. Bull. Volcanol. 70, 435–454.

Stern, C.R., Moreno, P.I., Henríquez, W.I., Villa-Martínez, R., Sagredo, E., Aravena, J.C., de Pol-Holz, R., 2016. Holocene tephrochronology around Cochrane (~ 47 S), southern Chile. Andean Geol. 43.

Stokes, C.R., Tarasov, L., Blomdin, R., Cronin, T.M., Fisher, T.G., Gyllencreutz, R., Hättestrand, C., Heyman, J., Hindmarsh, R.C.A., Hughes, A.L.C., Jakobsson, M., Kirchner, N., Livingstone, S.J., Margold, M., Murton, J.B., Noormets, R., Peltier, W.R., Peteet, D.M., Piper, D.J.W., Preusser, F., Renssen, H., Roberts, D.H., Roche, D.M., Saint-Ange, F., Stroeven, A.P., Teller, J.T., 2015. On the reconstruction of palaeo-ice sheets: Recent advances and future challenges. Quat. Sci. Rev. 125, 15–49. https://doi.org/http://dx.doi.org/10.1016/j.quascirev.2015.07.016

Thorndycraft, V.R., Bendle, J.M., Benito, G., Davies, B.J., Sancho, C., Palmer, A.P., Fabel, D., Medialdea, A., Martin, J.R. V, 2019. Glacial lake evolution and Atlantic-Pacific drainage reversals during deglaciation of the Patagonian Ice Sheet. Quat. Sci. Rev. 203, 102–127. https://doi.org/https://doi.org/10.1016/j.quascirev.2018.10.036

Tielidze, L.G., Wheate, R.D., 2018. The Greater Caucasus Glacier Inventory (Russia, Georgia and Azerbaijan). Cryosph. 12, 81–94. https://doi.org/10.5194/tc-12-81-2018

Timms, R.G.O., Matthews, I.P., Lowe, J.J., Palmer, A.P., Weston, D.J., MacLeod, A., Blockley, S.P.E., 2019. Establishing tephrostratigraphic frameworks to aid the study of abrupt climatic and glacial transitions: a case study of the Last Glacial-Interglacial Transition in the British Isles (c. 16-8 ka BP). Earth-Science Rev. https://doi.org/https://doi.org/10.1016/j.earscirev.2019.01.003

Tomkins, M.D., Dortch, J.M., Hughes, P.D., 2016. Schmidt Hammer exposure dating (SHED): Establishment and implications for the retreat of the last British Ice Sheet. Quat. Geochronol. 33, 46–60.

Tomkins, M.D., Dortch, J.M., Hughes, P.D., Huck, J.J., Tonkin, T.N., Barr, I.D., 2018a. Timing of glacial retreat in the Wicklow Mountains, Ireland, conditioned by glacier size and topography. J. Quat. Sci. 33, 611–623.

Tomkins, M.D., Huck, J.J., Dortch, J.M., Hughes, P.D., Kirbride, M.P., Barr, I.D., 2018b. Schmidt Hammer exposure dating (SHED): Calibration procedures, new exposure age data and an online calculator. Quat. Geochronol. 44, 55–62.

Warren, C., Benn, D., Winchester, V., Harrison, S., 2001. Buoyancy-driven lacustrine calving, Glaciar Nef, Chilean Patagonia. J. Glaciol. 47, 135–146. https://doi.org/10.3189/172756501781832403

Watson, E.J., Swindles, G.T., Lawson, I.T., Savov, I.P., 2016. Do peatlands or lakes provide the most comprehensive distal tephra records? Quat. Sci. Rev. 139, 110–128. https://doi.org/https://doi.org/10.1016/j.quascirev.2016.03.011

Weller, D.J., Miranda, C.G., Moreno, P.I., Villa-Martínez, R., Stern, C.R., 2015. Tephrochronology of the southernmost Andean southern volcanic zone, Chile. Bull. Volcanol. 77, 107.

White, T.S., Bridgland, D.R., Westaway, R., Straw, A., 2017. Evidence for late Middle Pleistocene glaciation of the British margin of the southern North Sea. J. Quat. Sci. 32, 261–275.

Wiles, G.C., Barclay, D.J., Calkin, P.E., 1999. Tree-ring-dated'Little Ice Age' histories of maritime glaciers from western Prince William Sound, Alaska. The Holocene 9, 163–173. https://doi.org/doi:10.1191/095968399671927145

Wiles, G.C., Lawson, D.E., Lyon, E., Wiesenberg, N., D'Arrigo, R.D., 2011. Tree-ring dates on two pre-Little Ice Age advances in Glacier Bay National Park and Preserve, Alaska, USA. Quat. Res. 76, 190–195. https://doi.org/http://dx.doi.org/10.1016/j.yqres.2011.05.005

Willis, M.J., Melkonian, A.K., Pritchard, M.E., Rivera, A., 2012. Ice loss from the Southern Patagonian Ice Field, South America, between 2000 and 2012. Geophys. Res. Lett. 39, L17501. https://doi.org/10.1029/2012gl053136

Wilson, P., Dunlop, P., Millar, C., Wilson, F.A., 2019. Age determination of glacially-transported boulders in Ireland and Scotland using Schmidt-hammer exposure-age dating (SHD) and terrestrial cosmogenic nuclide (TCN) exposure-age dating. Quat. Res. 1–13. https://doi.org/10.1017/qua.2019.12

Winchester, V., Harrison, S., 2000. Dendrochronology and lichenometry: colonization, growth rates and dating of geomorphological events on the east side of the North Patagonian Icefield, Chile. Geomorphology 34, 181–194. https://doi.org/10.1016/s0169-555x(00)00006-4

Winchester, V., Harrison, S., Warren, C.R., 2001. Recent retreat Glaciar Nef, Chilean Patagonia, dated by lichenometry and dendrochronology. Arct. Antarct. Alp. Res. 33, 266–273.

https://doi.org/10.2307/1552233

Winchester, V., Sessions, M., Cerda, J.V., Wündrich, O., Clemmens, S., Glasser, N.F., Nash, M., 2014. Post-1850 changes in Glacier Benito, North Patagonian Icefield, Chile. Geogr. Ann. Ser. A, Phys. Geogr. 96, 43–59. https://doi.org/10.1111/geoa.12027

Winkler, S., 2014. Investigation of late-Holocene moraines in the western Southern Alps, New Zealand, applying Schmidt-hammer exposure-age dating. The Holocene 24, 48–66.

Winkler, S., 2009. First attempt to combine terrestrial cosmogenic nuclide (^{10}Be) and Schmidt hammer relative-age dating: Strauchon Glacier, Southern Alps, New Zealand. Cent. Eur. J. Geosci. 1, 274–290.

Winkler, S., Matthews, J.A., 2016. Inappropriate instrument calibration for Schmidt-hammer exposure-age dating (SHD) – A comment on Dortch et al., Quaternary Geochronology 35 (2016), 67–68. Quat. Geochronol. 36, 102–103. https://doi.org/https://doi.org/10.1016/j.quageo.2016.08.009

Zolitschka, B., Francus, P., Ojala, A.E.K., Schimmelmann, A., 2015. Varves in lake sediments–a review. Quat. Sci. Rev. 117, 1–41.

Zumbühl, H.J., Steiner, D., Nussbaumer, S.U., 2008. 19th century glacier representations and fluctuations in the central and western European Alps: An interdisciplinary approach. Glob. Planet. Change 60, 42–57.